

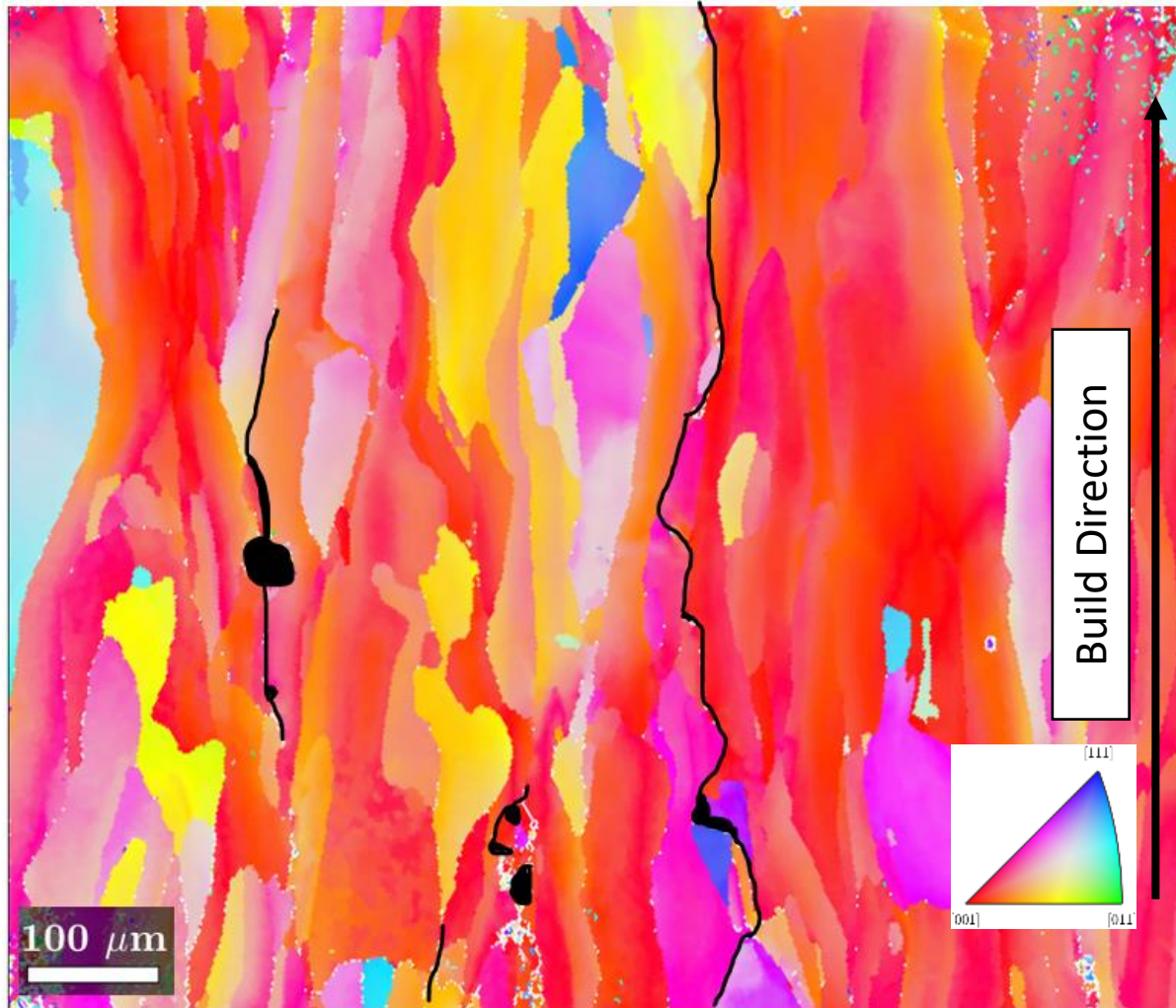
---

***Project 30-L: Mechanisms of Grain Refinement in Laser Powder  
Bed Fusion of In-Situ Metal Matrix Composite 6061 Aluminum  
Alloys***

***Spring Meeting  
April 12, 2022***

- Student: Chloe Johnson
- Advisor: Dr. Amy Clarke
- Thesis Committee: Dr. Kester Clarke, Dr. Michael Kaufman, Dr. Jeremy Iten, Dr. Garritt Tucker

# Project Motivation

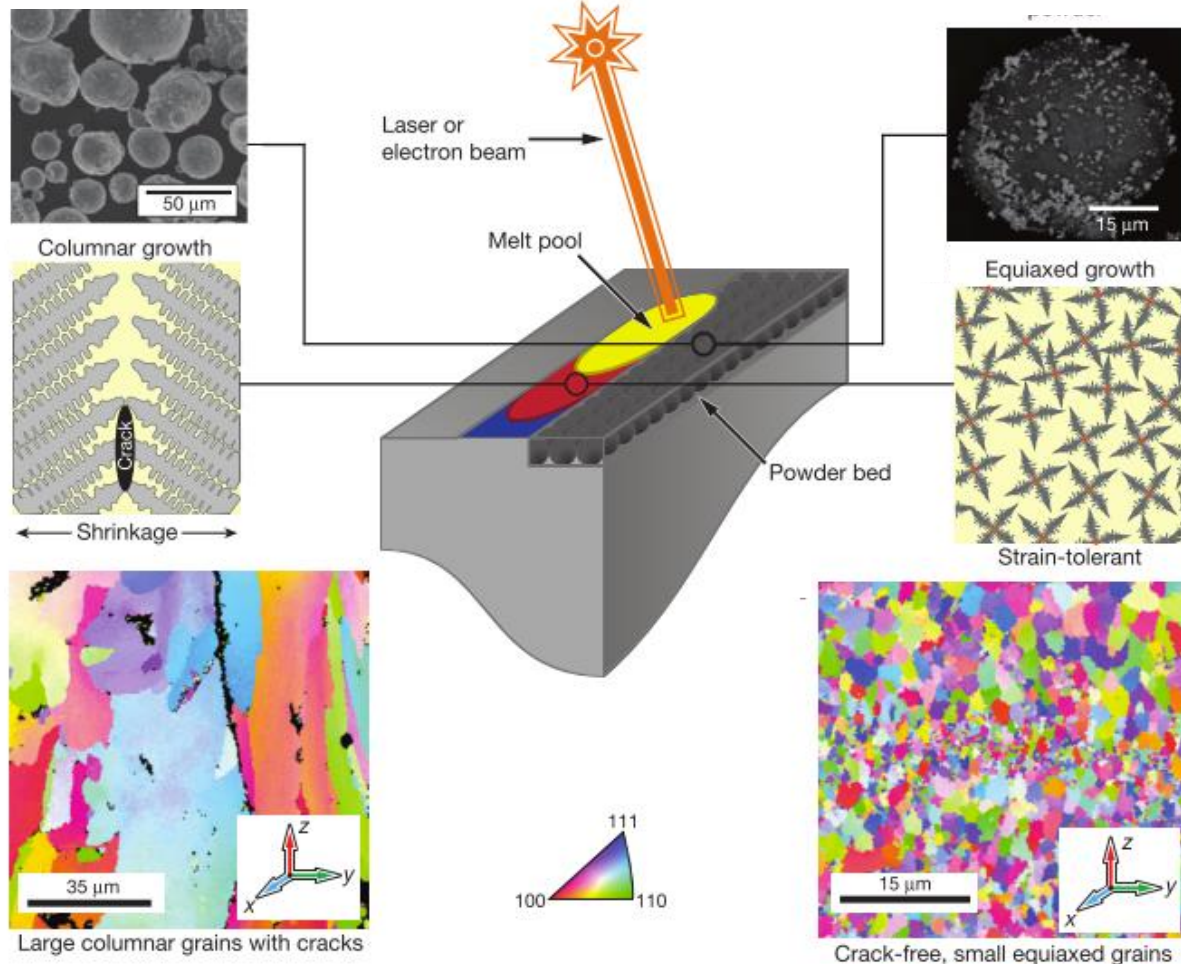


Inverse pole figure of 3D-printed stock 6061, black regions show areas of observed solidification cracking in SEM imaging

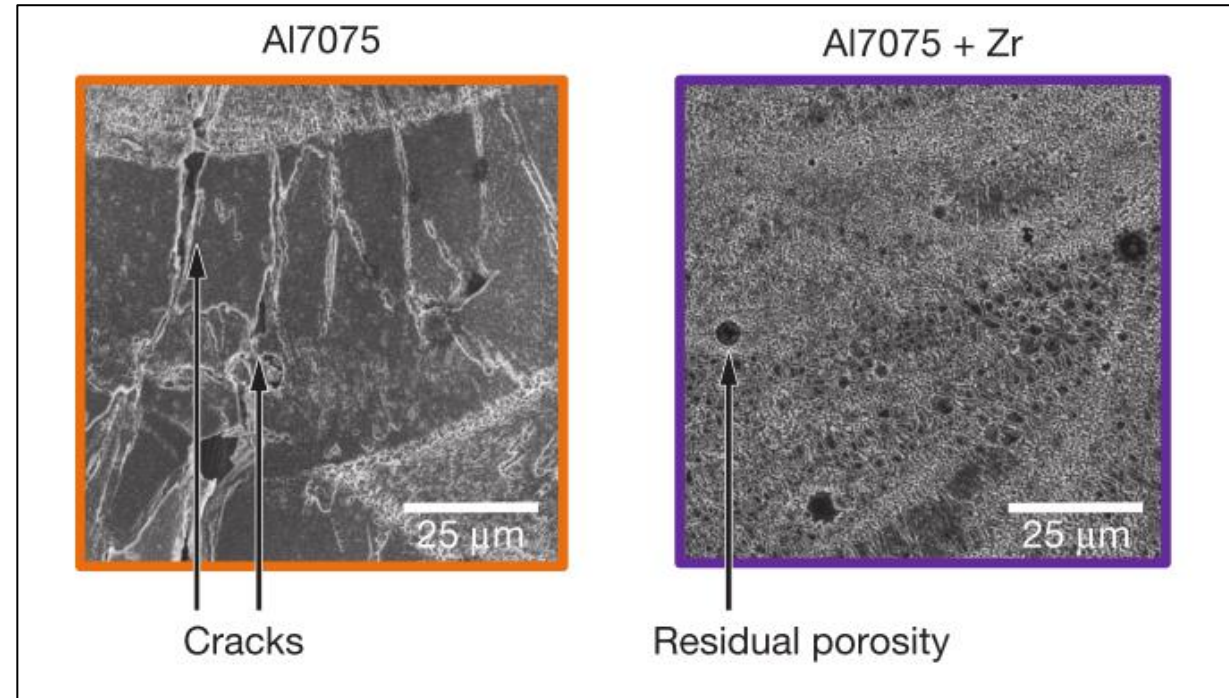
- AM presents method to print new geometries, like complex cooling channels, allowing for use of lower operating temperature alloys like Al alloys
- Al alloys currently used in AM are limited, and have mostly been casting alloys (e.g. AlSi10Mg)
- Under AM conditions, many Al alloys tend to form columnar grains, and are subject to solidification cracking
- These results imply a need for Al alloys designed specifically for AM

# Grain Size Control via Inoculants in AM Alloy Powders

## Standard Alloys

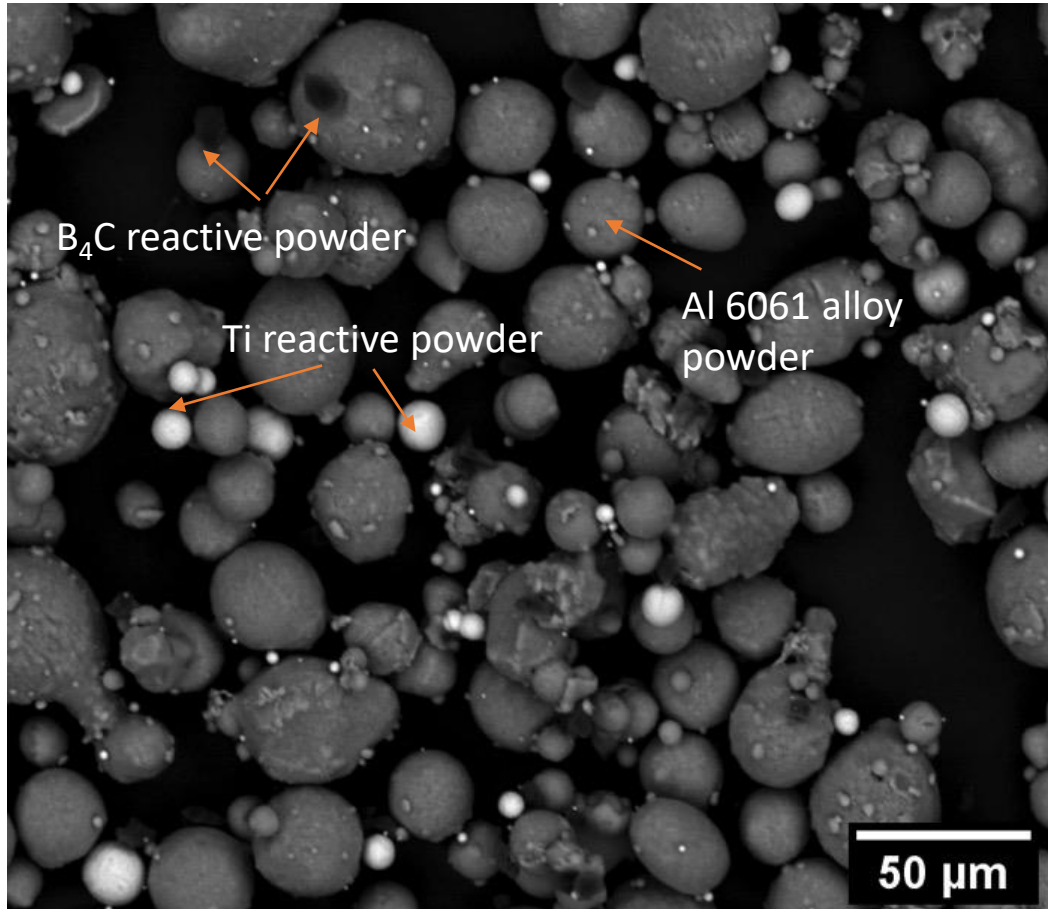


## Inoculated Alloys

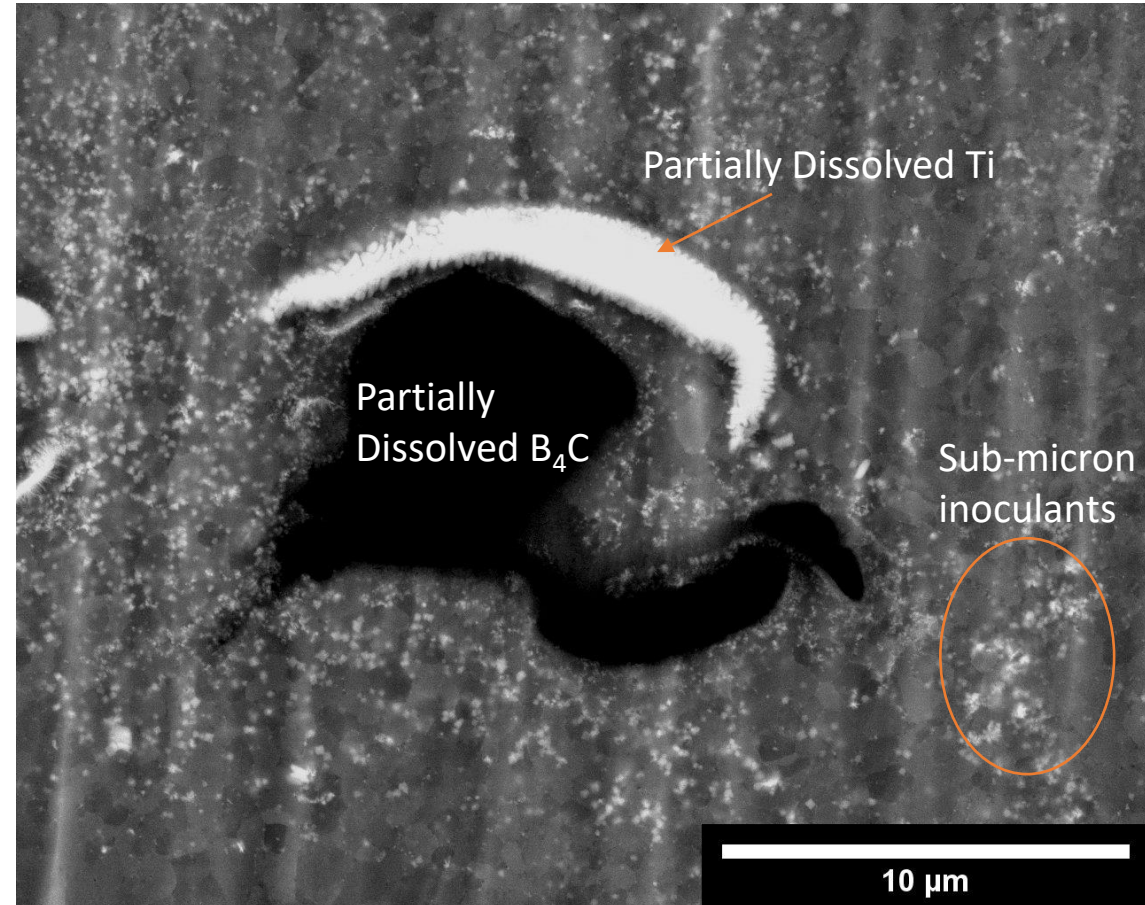


Taken from: Martin et. al, 3D Printing of High-Strength Aluminium Alloys, Nature (2017).

# A6061 Reactive Additive Manufacturing (RAM) Alloy Designed for AM



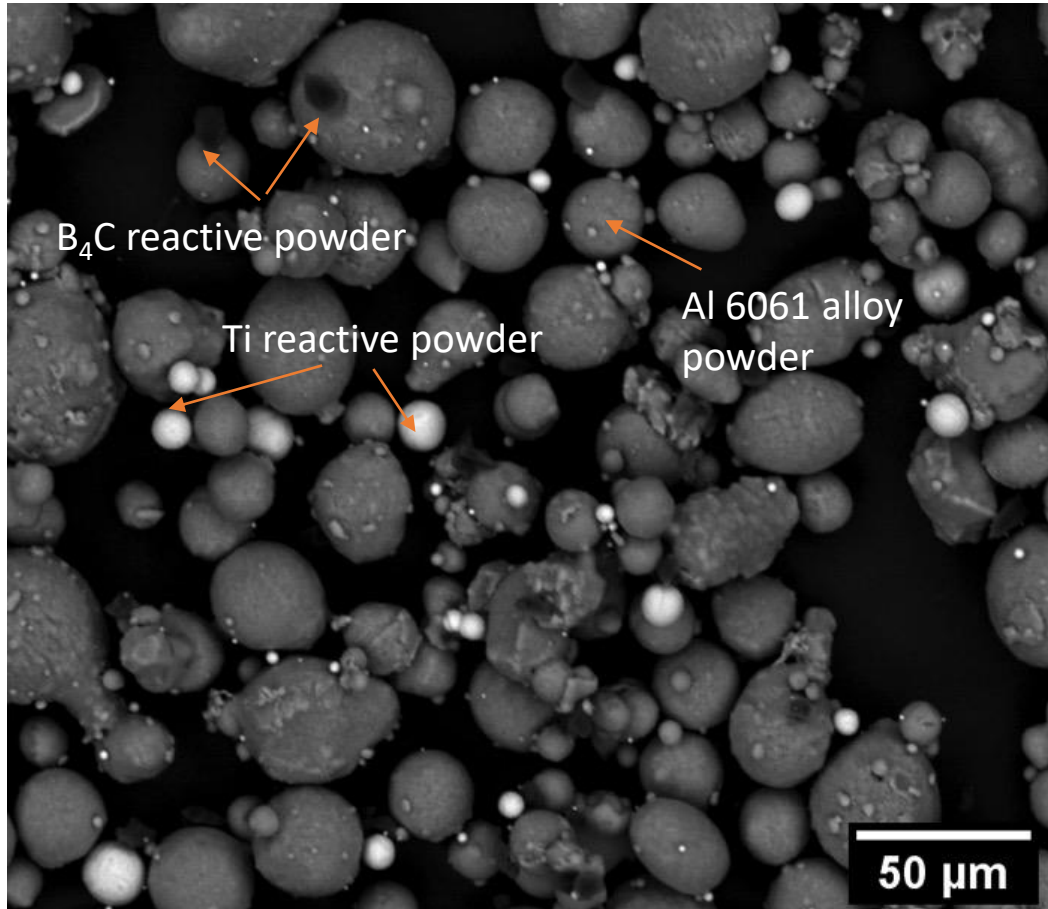
BSE SEM image of A6061-RAM2 alloy powder, 2 refers to vol. % of Ti and B<sub>4</sub>C in a ratio of 3:1



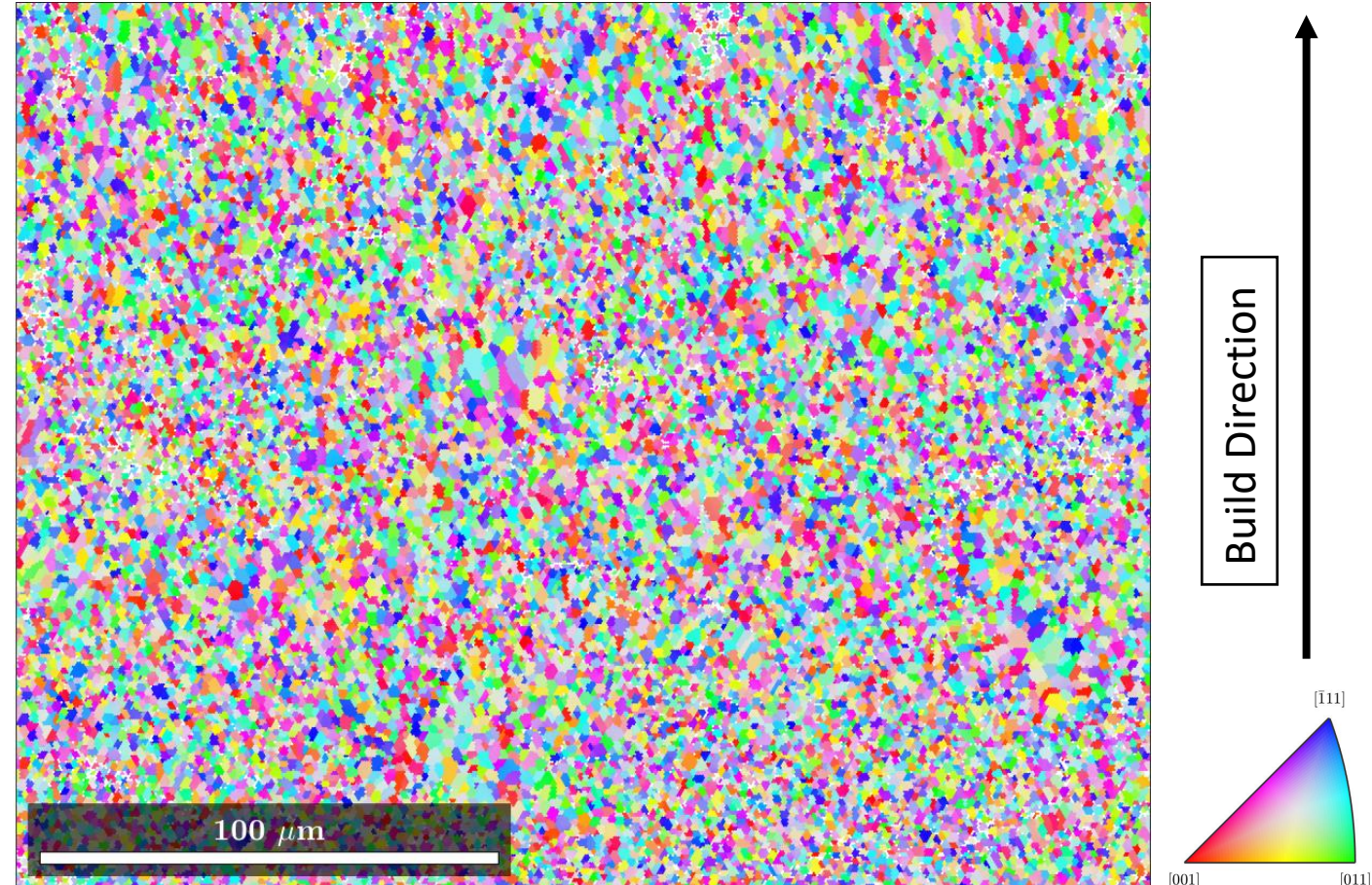
SEM back scatter image of as built A6061-RAM2

J. S. Neuchterlein & J. J. Iten, Reactive additive manufacturing, US Patent 20160271878 A1, priority 2015-03-17, published 2016-10-22.

# Al 6061 Reactive Additive Manufacturing (RAM) Alloy Designed for AM



BSE SEM image of A6061-RAM2 alloy powder, 2 refers to vol. % of Ti and B<sub>4</sub>C in a ratio of 3:1



EBSD IPF of as built A6061-RAM2

J. S. Neuchterlein & J. J. Iten, Reactive additive manufacturing, US Patent 20160271878 A1, priority 2015-03-17, published 2016-10-22.

# Project Objectives/Research Questions



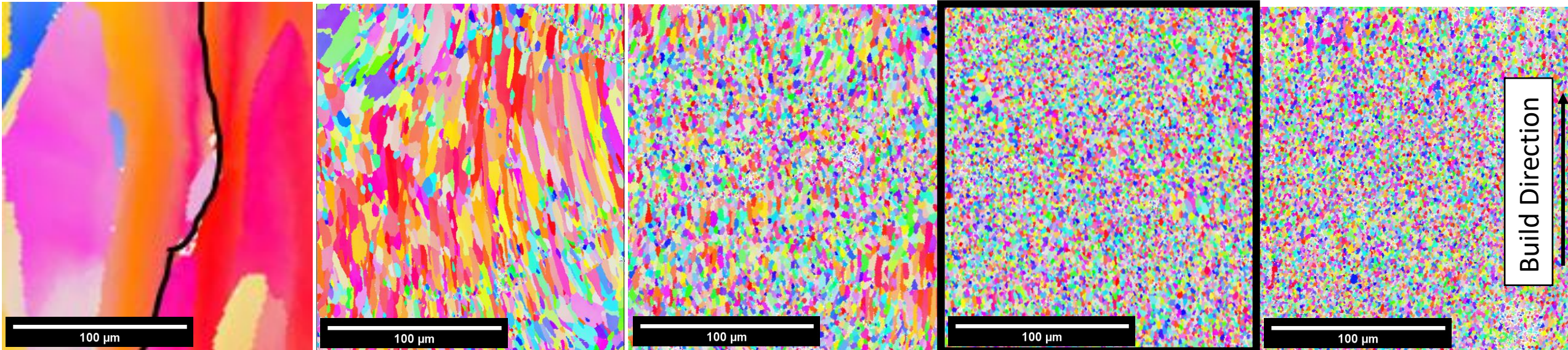
1. How do solidification conditions, specifically solidification velocity and thermal gradient, impact grain refinement mechanisms in A6061-RAM alloys during laser powder bed processing?
2. How does starting reactive particle content in A6061-RAM alloys impact inoculant formation and grain refinement mechanisms during laser powder bed fusion?
3. What is the impact of particle content in as-built A6061-RAM alloys, built using laser powder bed fusion, on aging and precipitation strengthening in these alloys?

## Research Question 2

How does starting reactive particle content in A6061-RAM alloys impact inoculant formation and grain refinement mechanisms during laser powder bed fusion?

- Varied starting reactive particle content for samples containing both Ti and  $B_4C$  (0.5, 1, 2, 10 vol. %)
- Isolated impacts of Ti vs.  $B_4C$  on refinement
- Characterized grain structure and particle content in all alloys

# Degree of Refinement for Various Starting Reactive Particle Content



**6061**  
Grain size  
Area:  $291.38 \mu\text{m}^2$   
Diameter:  $12.59 \mu\text{m}$   
(range of  $2.31\text{-}941.19 \mu\text{m}$   
max diameter)

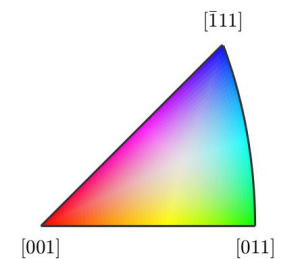
**RAM 0.5**  
Grain size  
Area:  $8.87 \mu\text{m}^2$   
Diameter:  $4.37 \mu\text{m}$

**RAM 1**  
Grain size  
Area:  $3.84 \mu\text{m}^2$   
Diameter:  $2.80 \mu\text{m}$

**RAM 2**  
Grain size  
Area:  $1.91 \mu\text{m}^2$   
Diameter:  $1.93 \mu\text{m}$

**RAM 10**  
Grain size  
Area:  $1.74 \mu\text{m}^2$   
Diameter:  $1.87 \mu\text{m}$

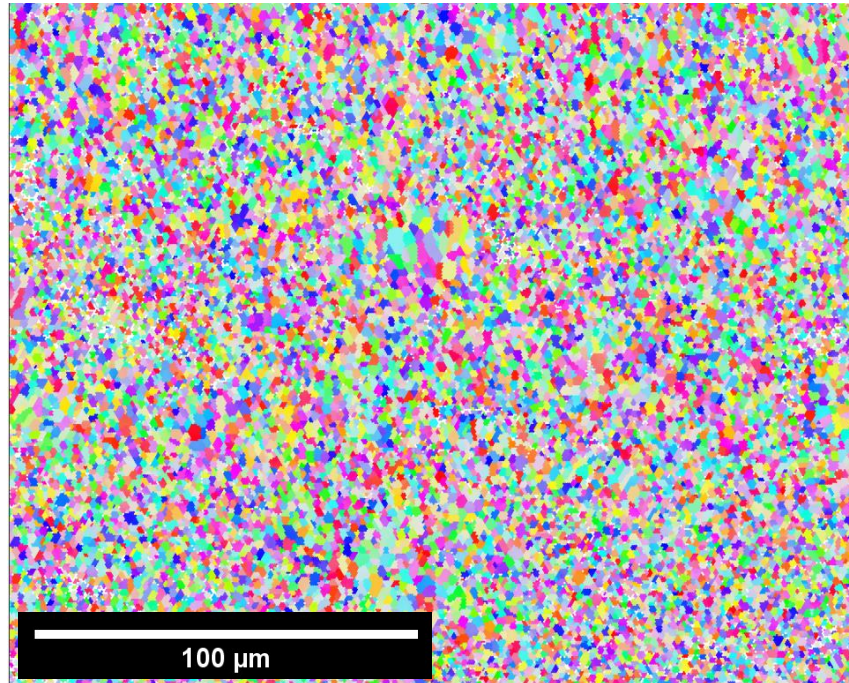
Increasing RAM Content →



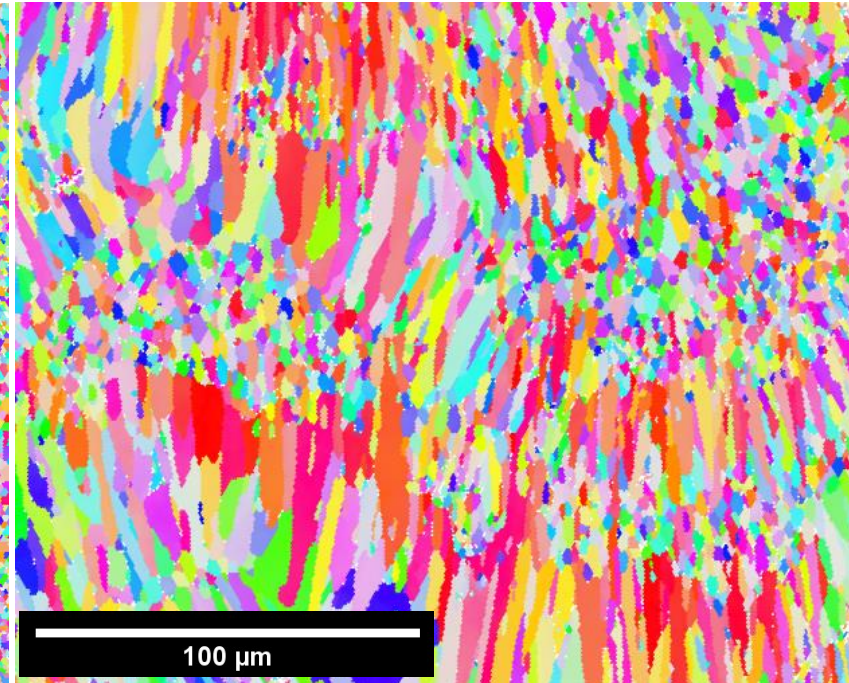


# Impact of Individual Reactive Powders ( $B_4C$ or Ti) vs. A6061-RAM2 ( $B_4C + Ti$ )

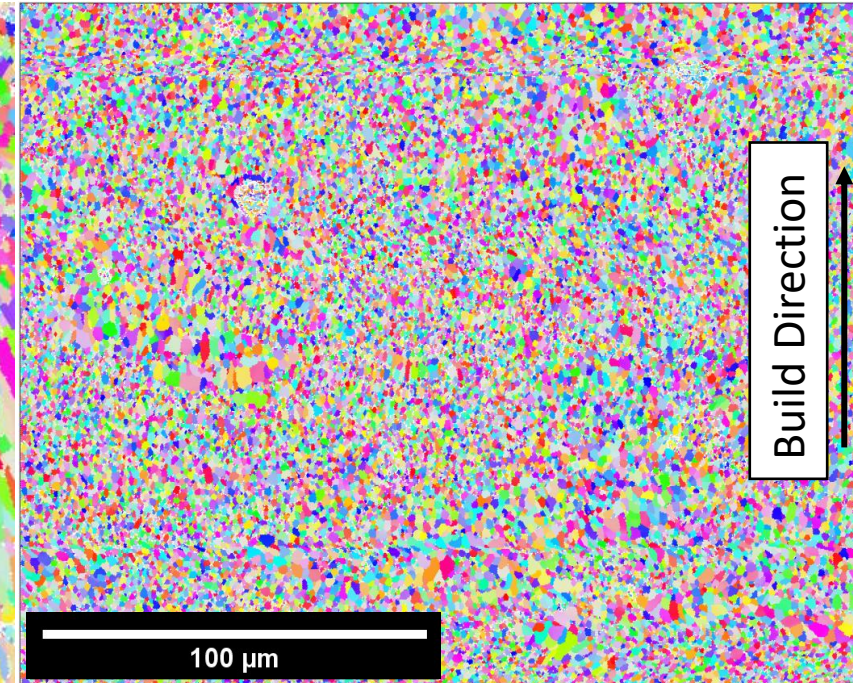
All builds were performed with 40  $\mu m$  layer thickness, 370 W, 0.2 mm hatch spacing



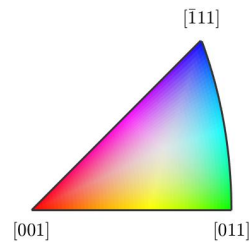
**A6061-RAM2**  
1300 mm/s  
Grain size  
Area:  $1.95 \mu m^2$   
Diameter:  $1.96 \mu m$



**A6061-RAM:  $B_4C$**   
1300 mm/s  
Grain size  
Area:  $9.65 \mu m^2$   
Diameter:  $4.81 \mu m$



**A6061-RAM: Ti**  
1300 mm/s  
Grain size  
Area:  $0.73 \mu m^2$   
Diameter:  $1.16 \mu m$

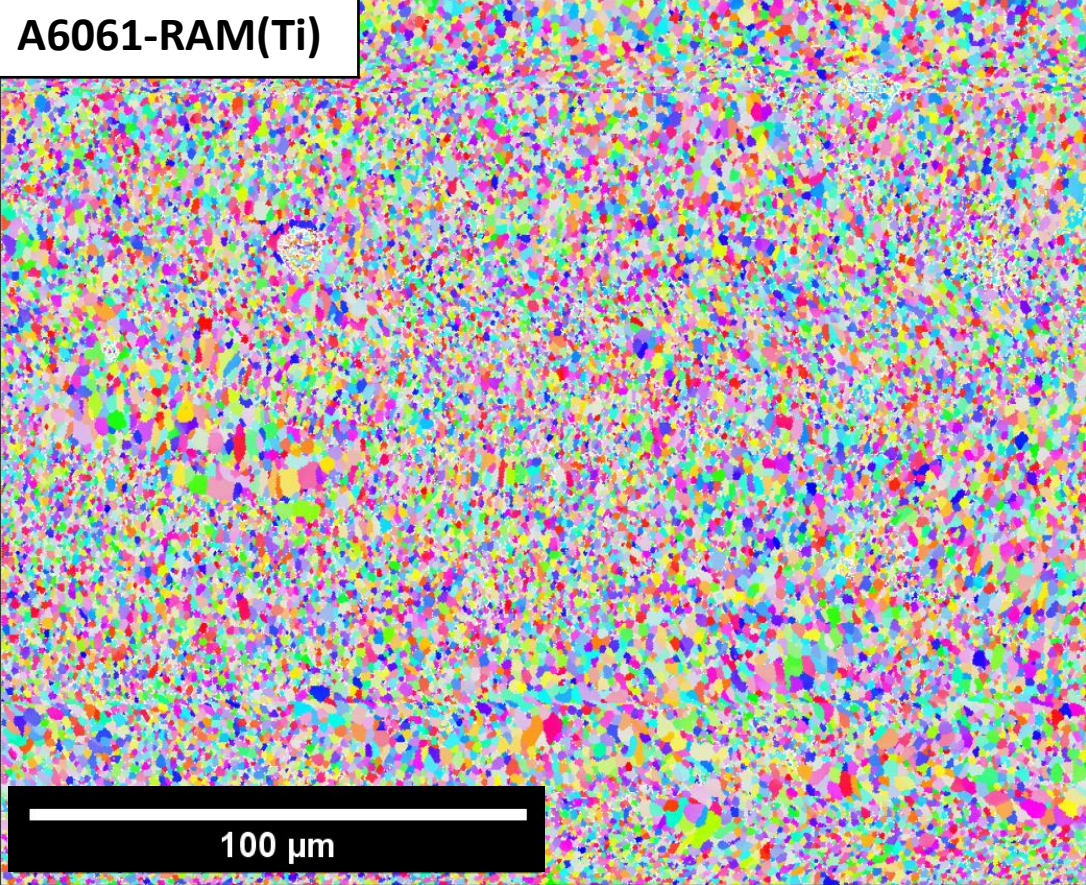


# Comparison of Grain Structure A6061-RAM(Ti) vs. Al-Ti

40  $\mu\text{m}$  layer thickness, 370 W, 1300 mm/s, and 0.2 mm hatch spacing

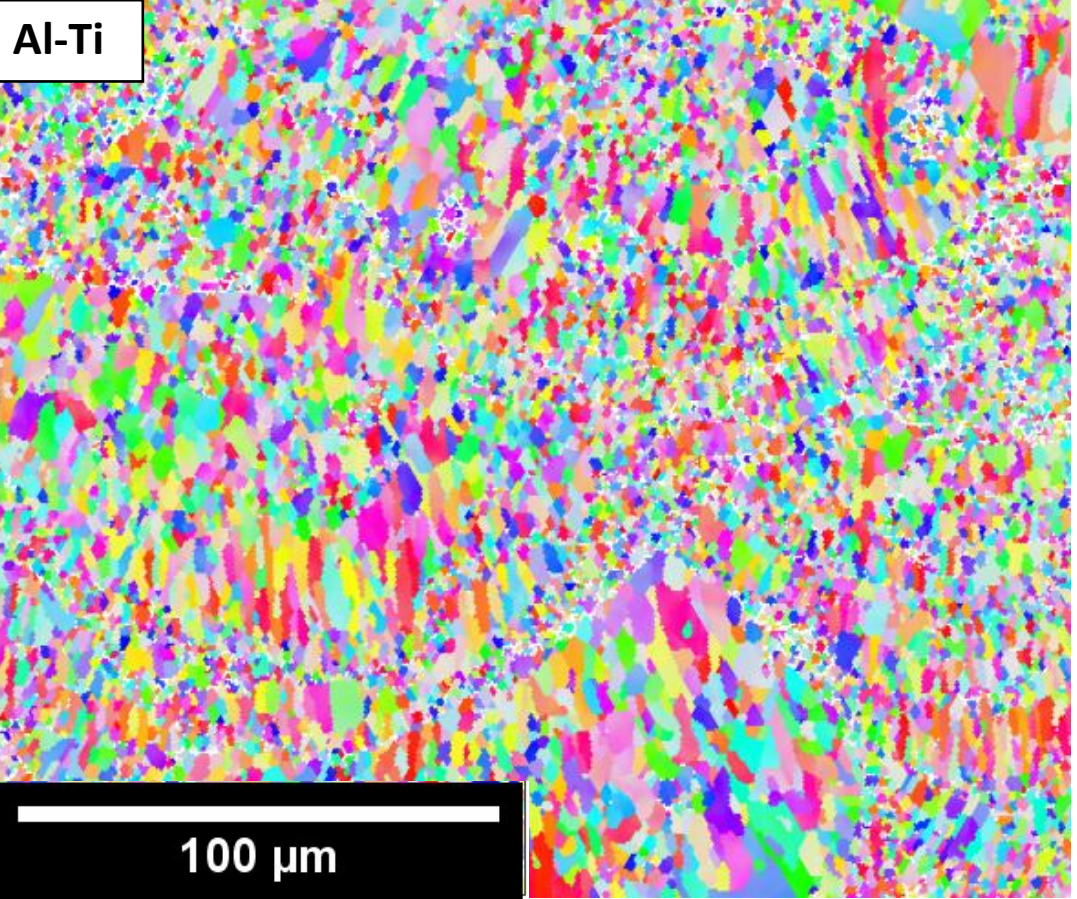
30  $\mu\text{m}$  layer thickness, 370 W, 1300 mm/s, and 0.19 mm hatch spacing

A6061-RAM(Ti)



Grain size  
Area:  $0.73 \mu\text{m}^2$   
Diameter:  $1.16 \mu\text{m}$

Al-Ti



Grain size  
Area:  $2.83 \mu\text{m}^2$   
Diameter:  $2.32 \mu\text{m}$

Build Direction

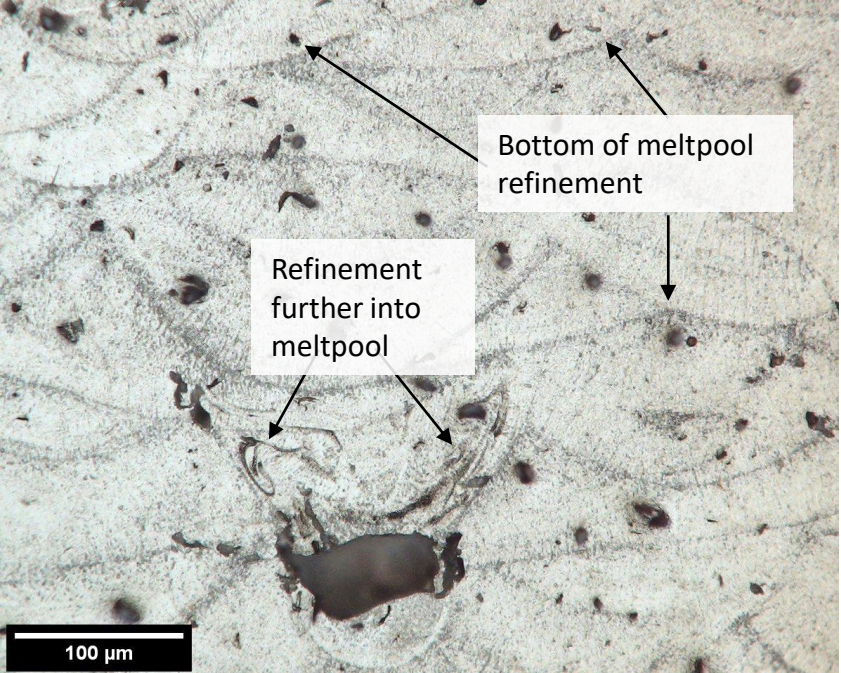
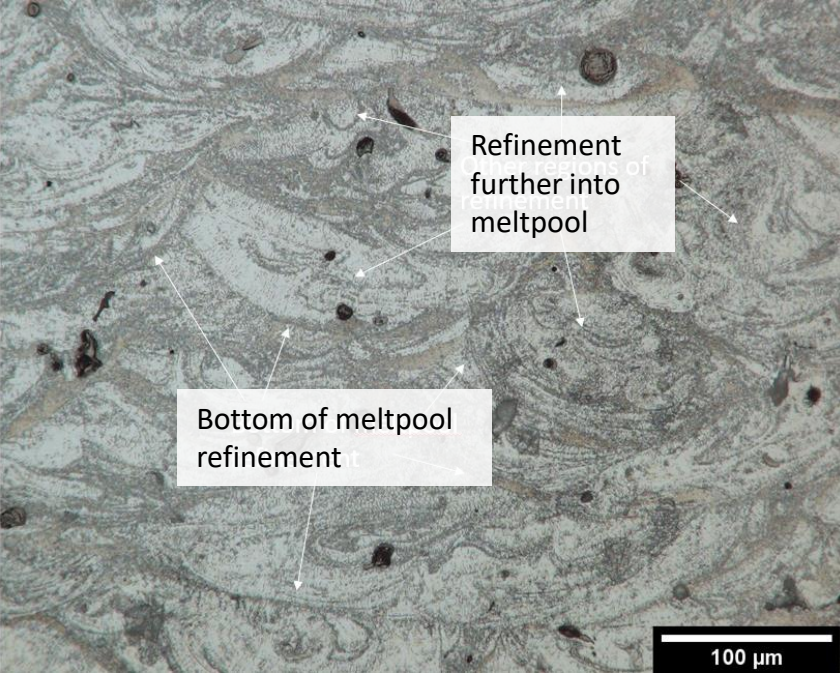
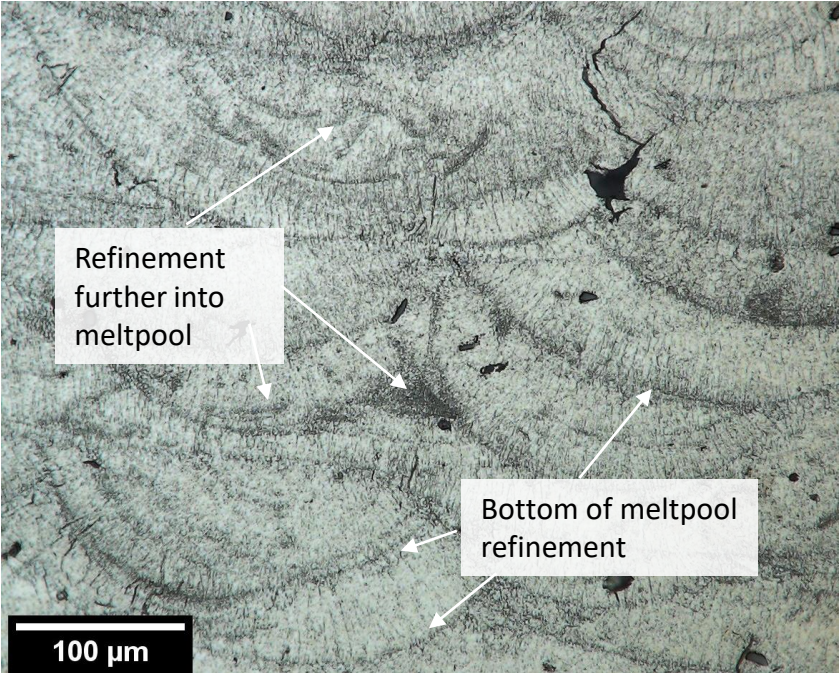


# Refinement Locations in Samples with a CET

A6061-RAM0.5

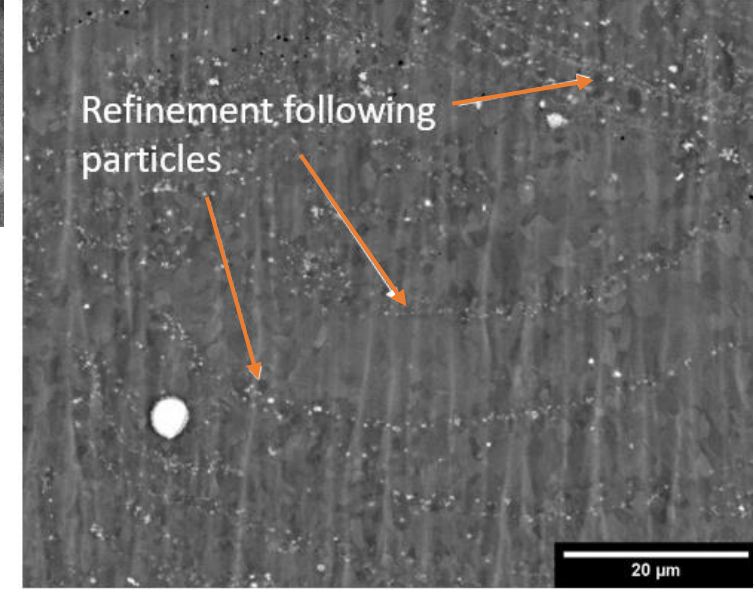
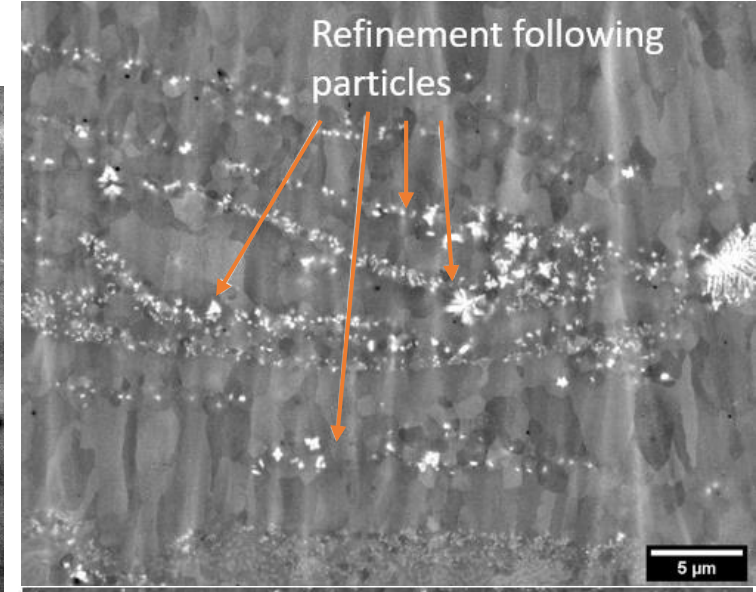
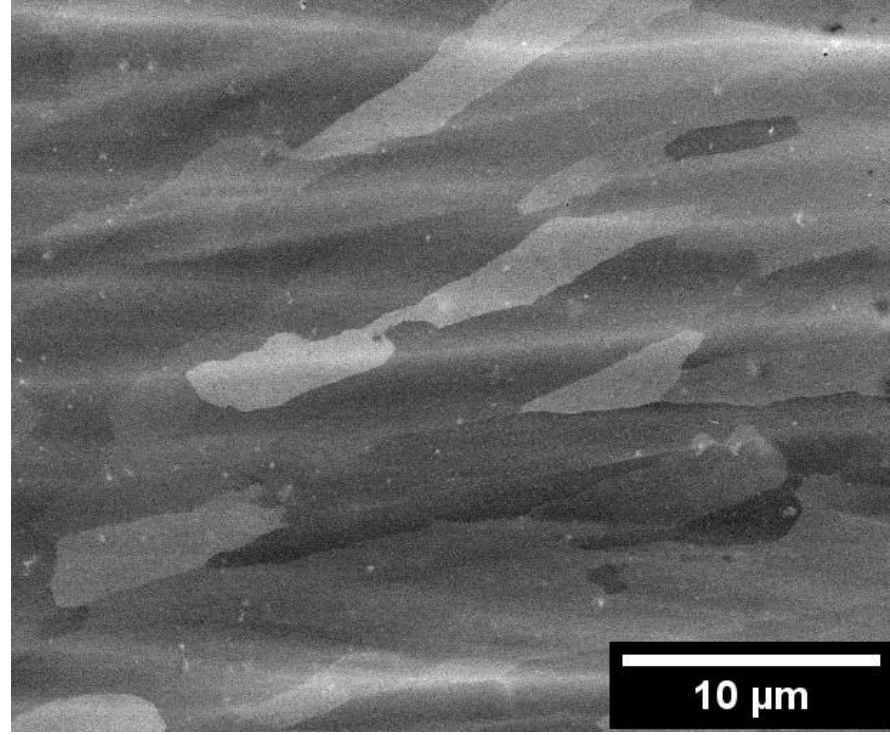
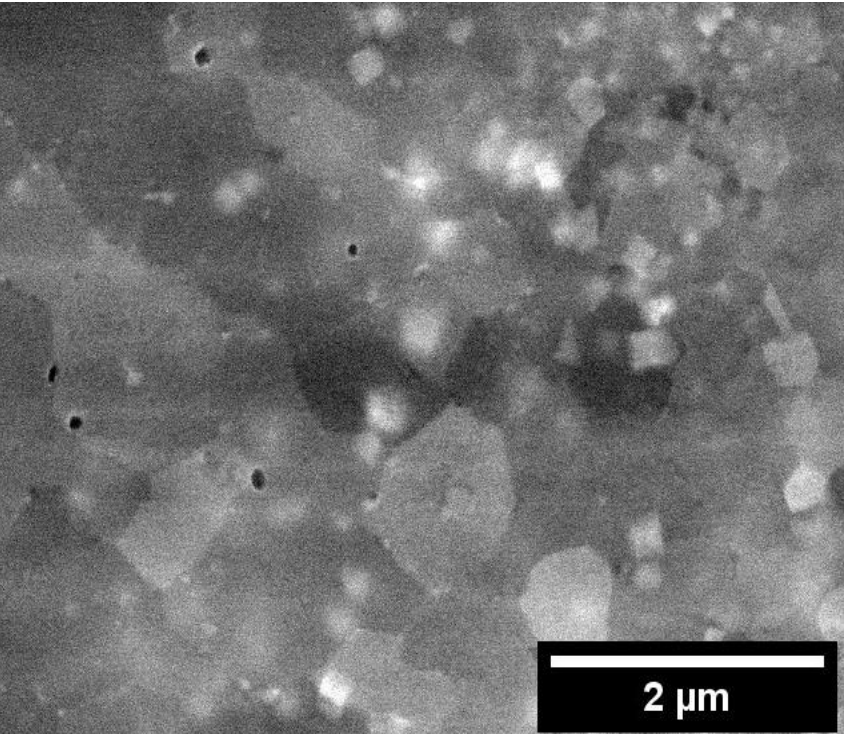
Al-Ti

A6061-RAM(B<sub>4</sub>C)



Light optical microscopy (LOM) images of samples etched with Kroll's Reagent

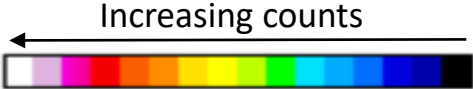
# Refined vs. Columnar Regions: SEM Observations



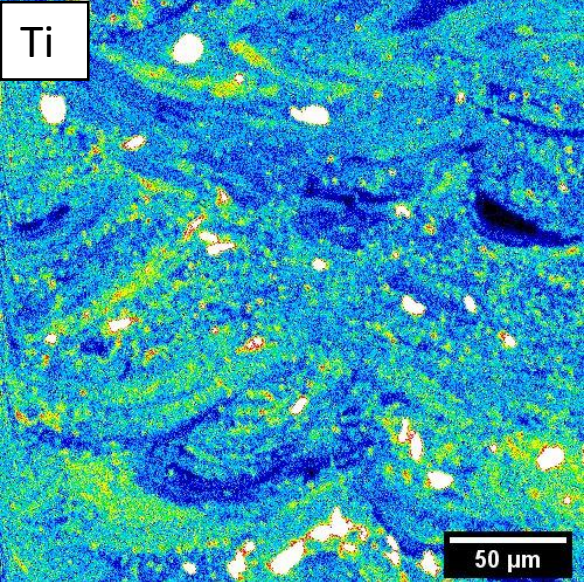
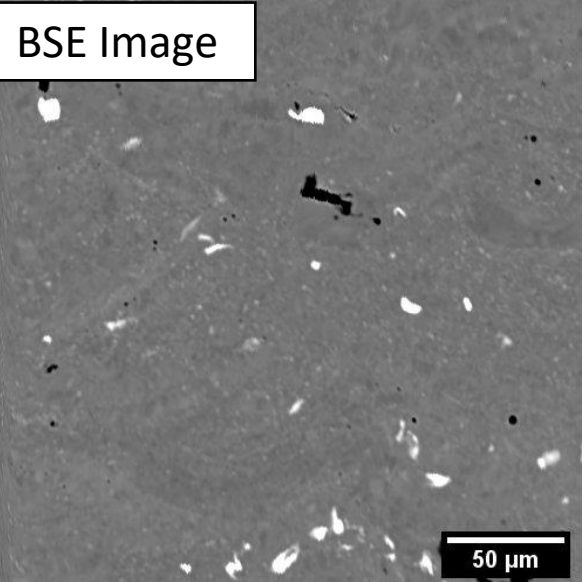
SEM-BSE Images taken from an A6061-RAM0.5 sample

SEM-BSE Images taken from an Al-Ti sample

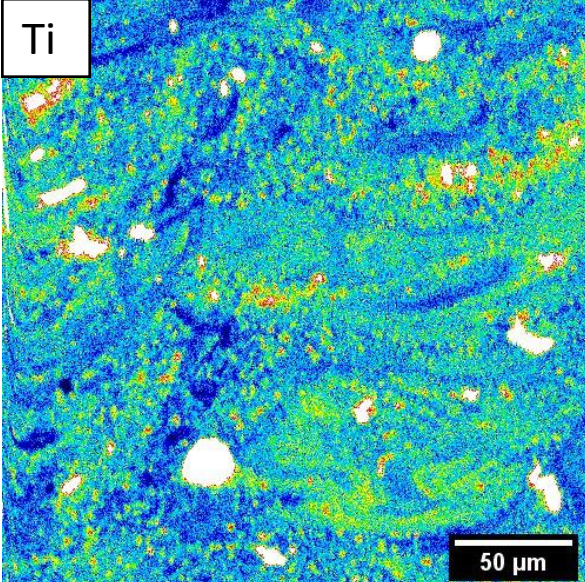
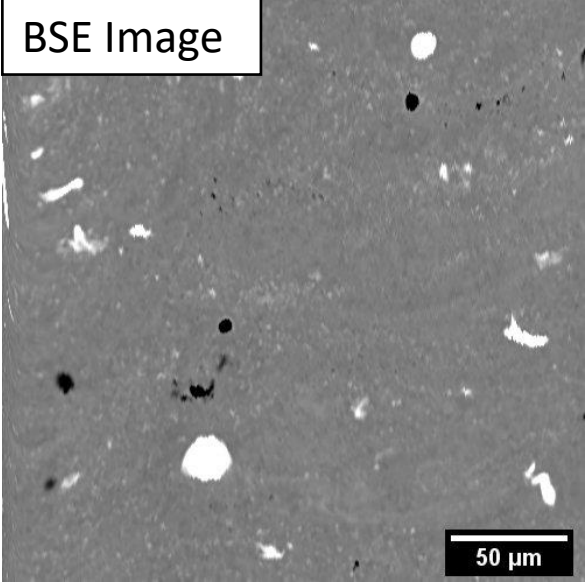
# Electron Microprobe Maps of Solute Distribution



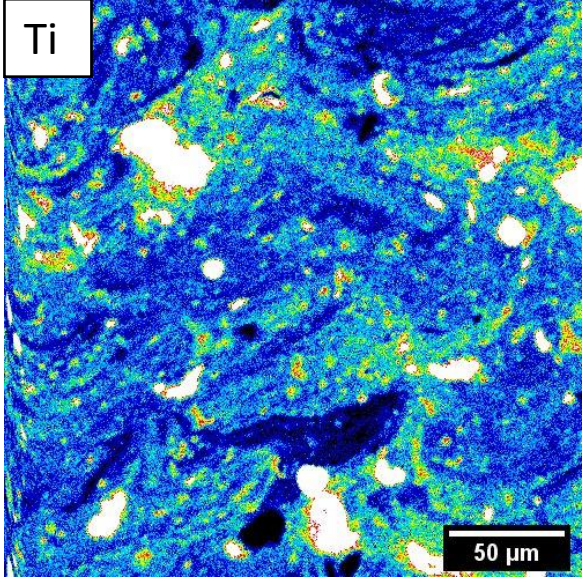
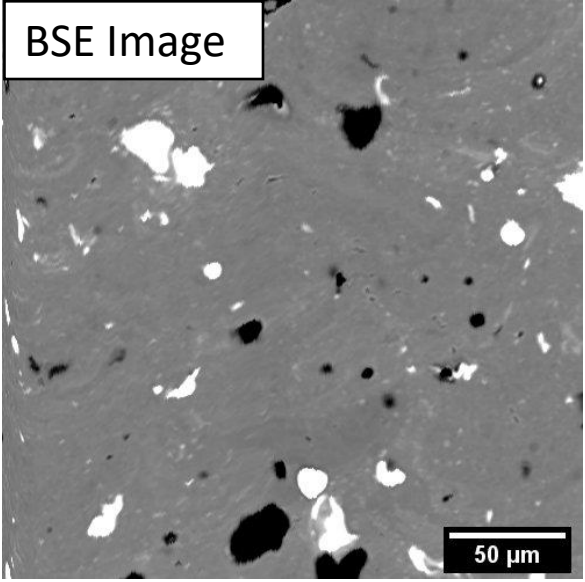
A6061-RAM2



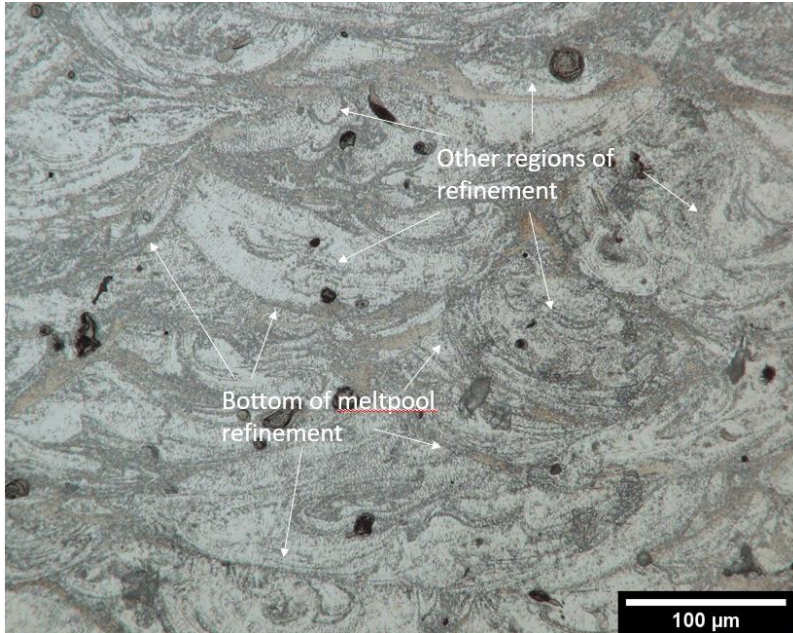
A6061-RAM(Ti)



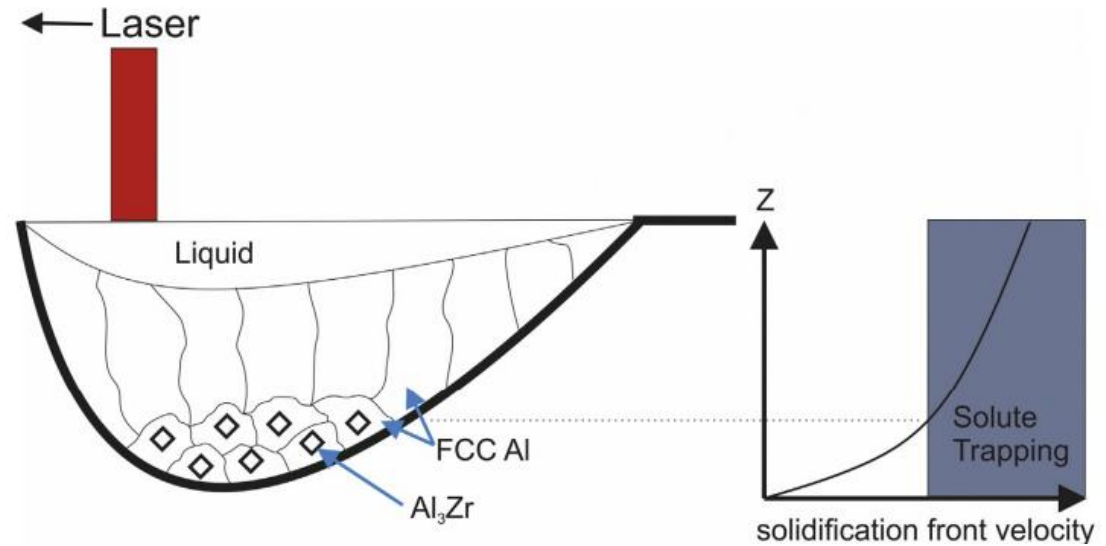
Al-Ti



# Factors Contributing to Refinement Locations: Bottom of the Melt Pool



LOM of etched Al-Ti as-built sample



Taken from: Griffiths et. al, Effect of laser rescanning on the grain microstructure of a selective laser melted Al-Mg-Zr alloy, Materials Characterization (2018).

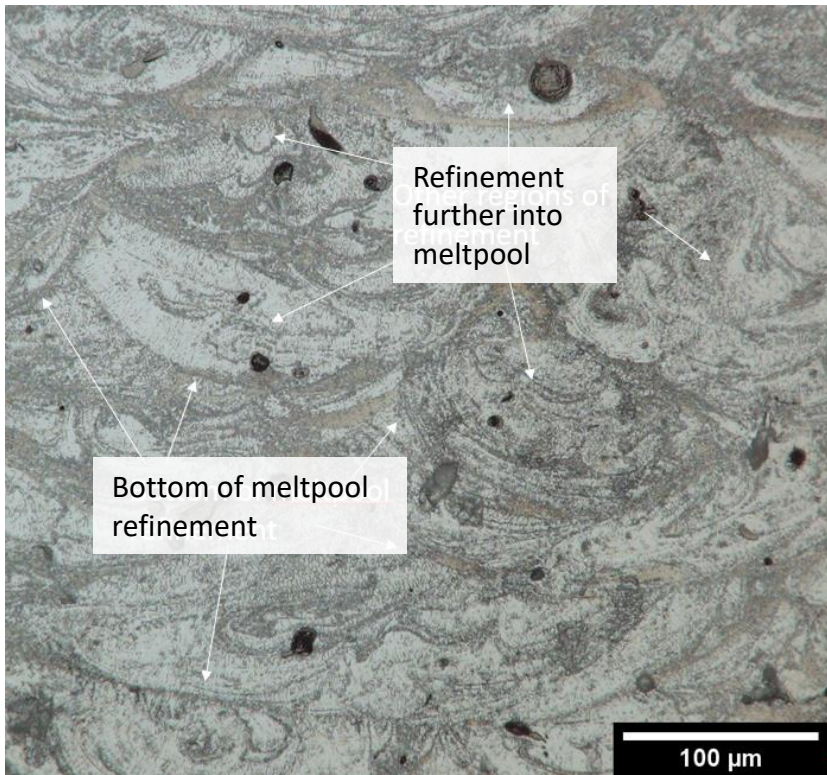
## Nominal and measured (STEM EDS) Ti content for various alloys

Sample	Measured Ti (wt. %)	Nominal Ti (wt. %)
Al-Ti	0.96 $\pm$ 0.46	2.45
A6061-RAM(Ti)	0.8 $\pm$ 0.42	2.45
A6061-RAM2	1.12 $\pm$ 0.41	2.45
A6061-RAM10	0.69 $\pm$ 0.22	12.25

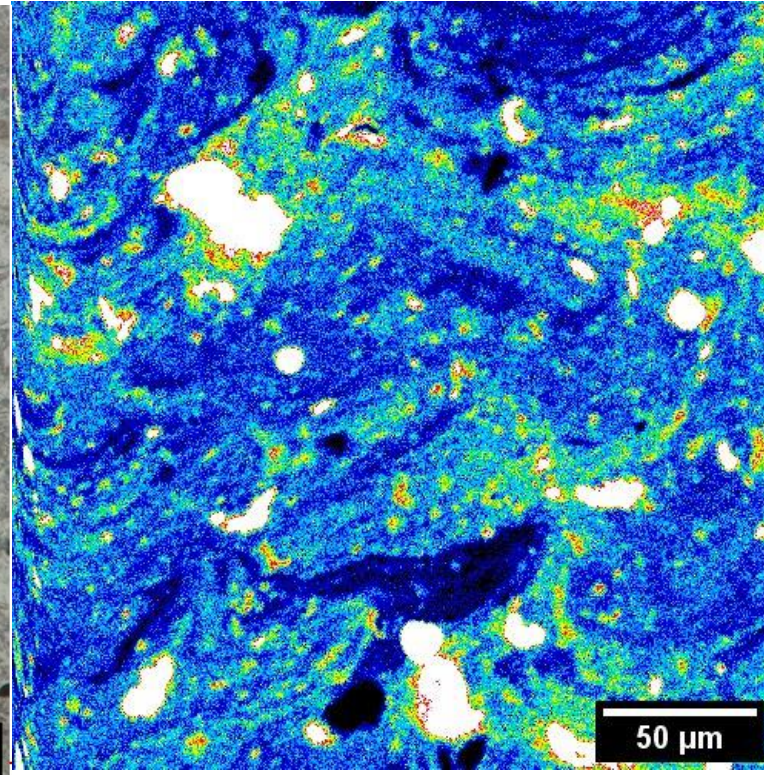
Note: maximum solubility of Ti in Al  $\sim$  1.1 wt.%

# Factors Contributing to Refinement Locations: Further into the Meltpool

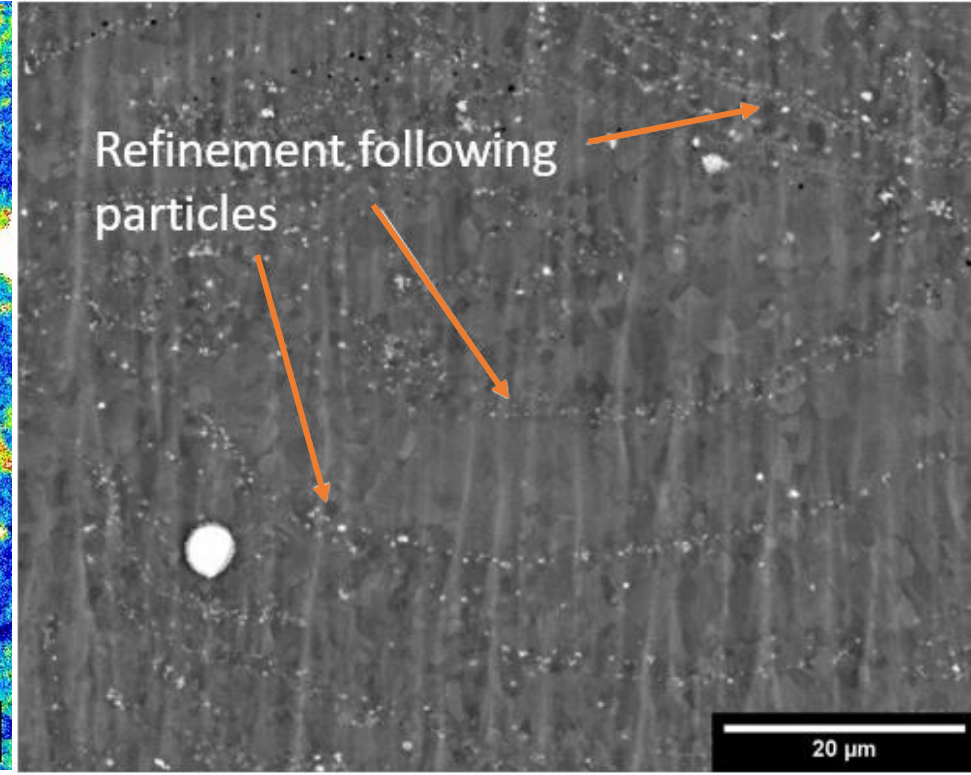
Al-Ti



Etched LOM Image

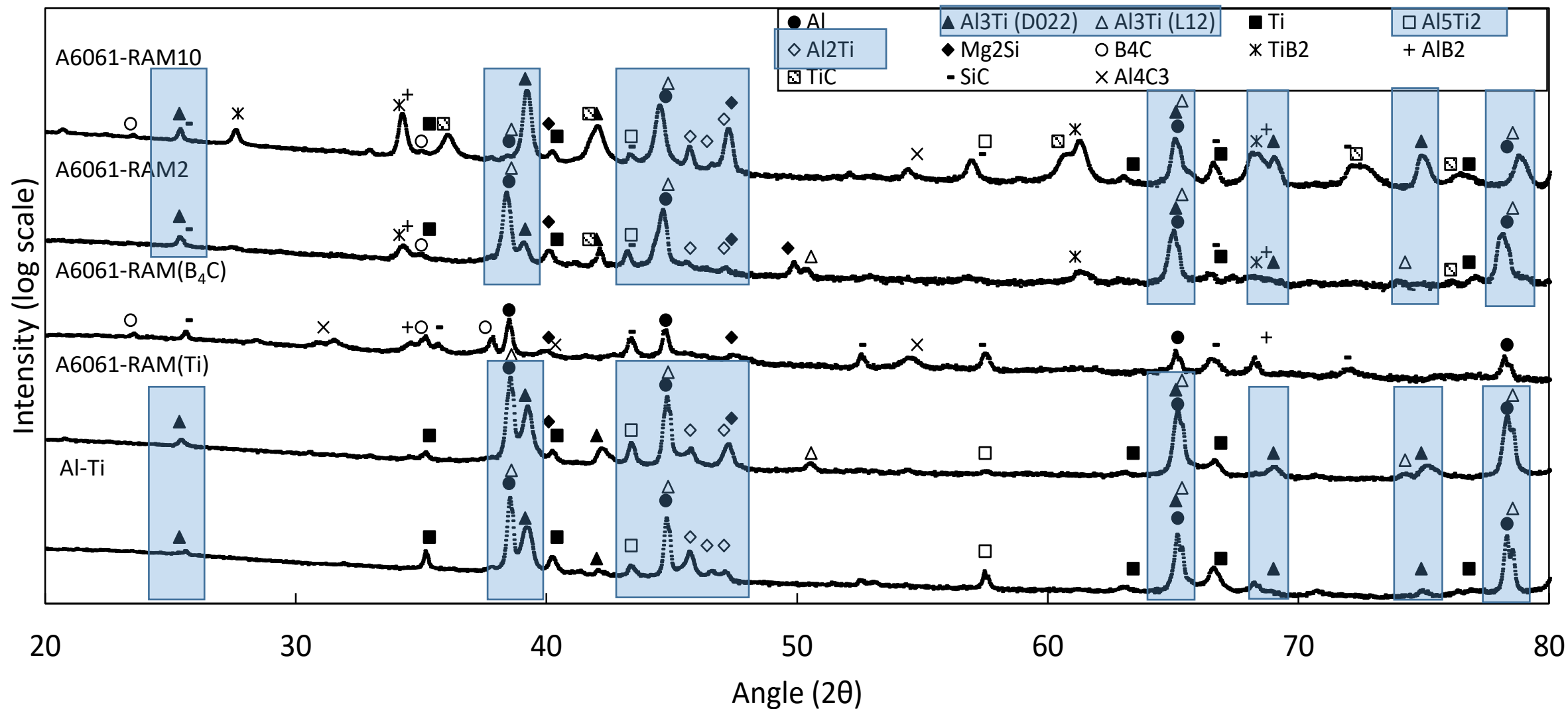


EPMA Ti map



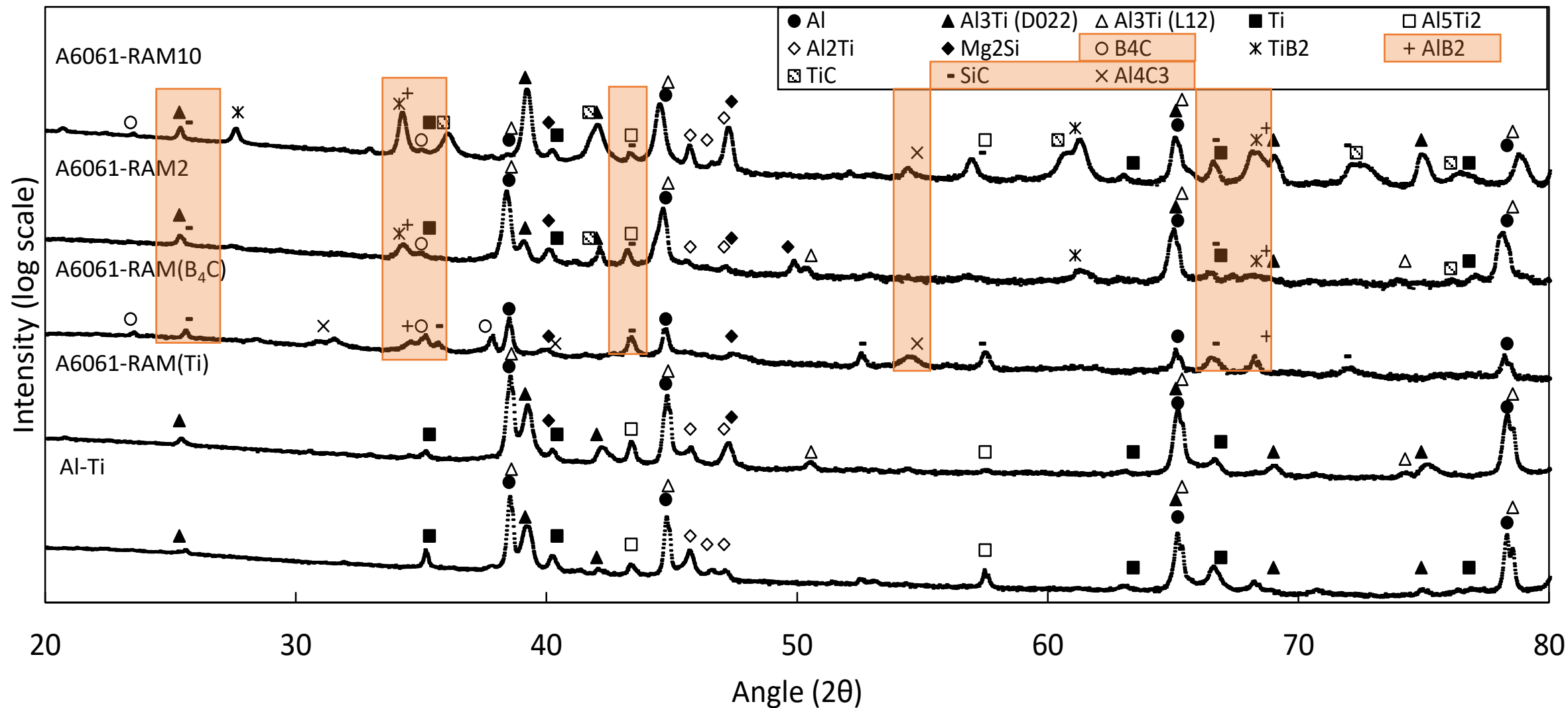
SEM BSE Image

# Particle Types (XRD) For Dissolved Matrix Samples

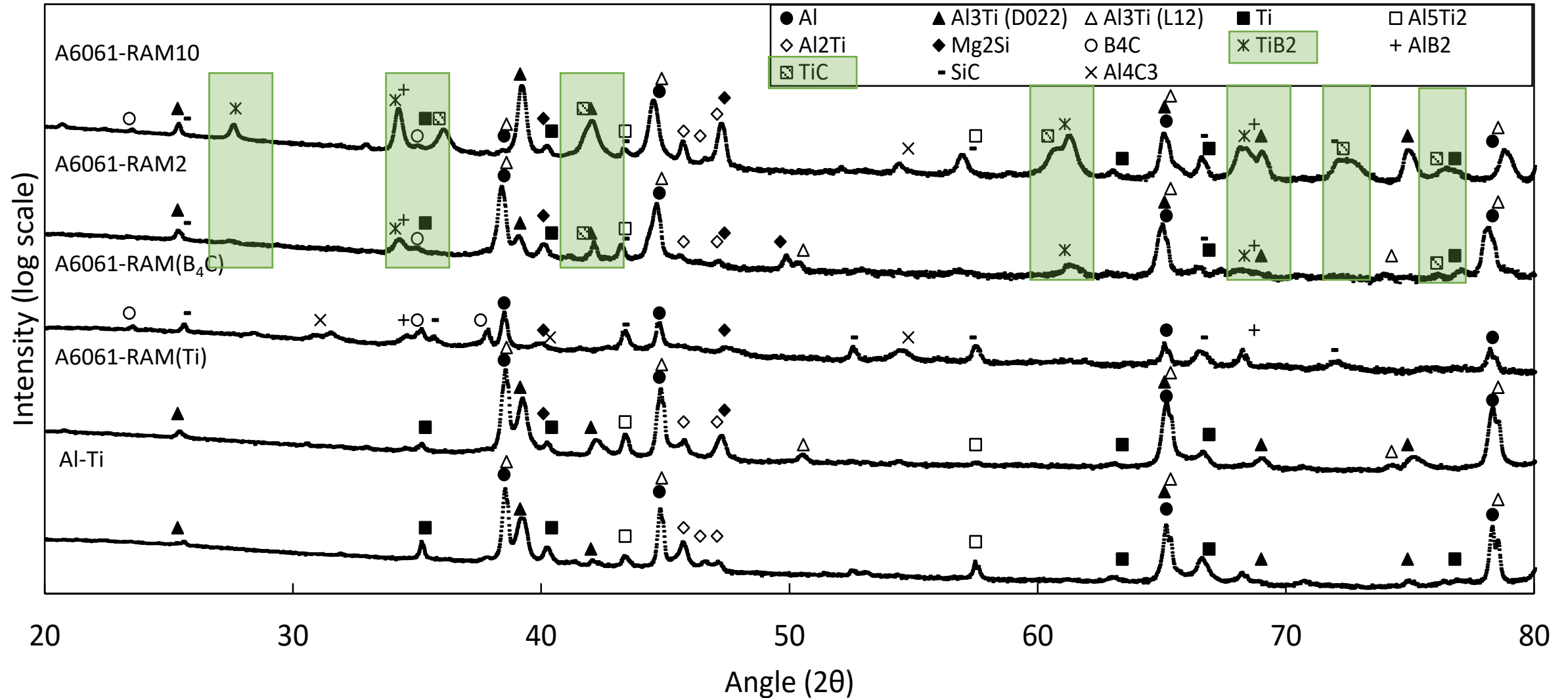




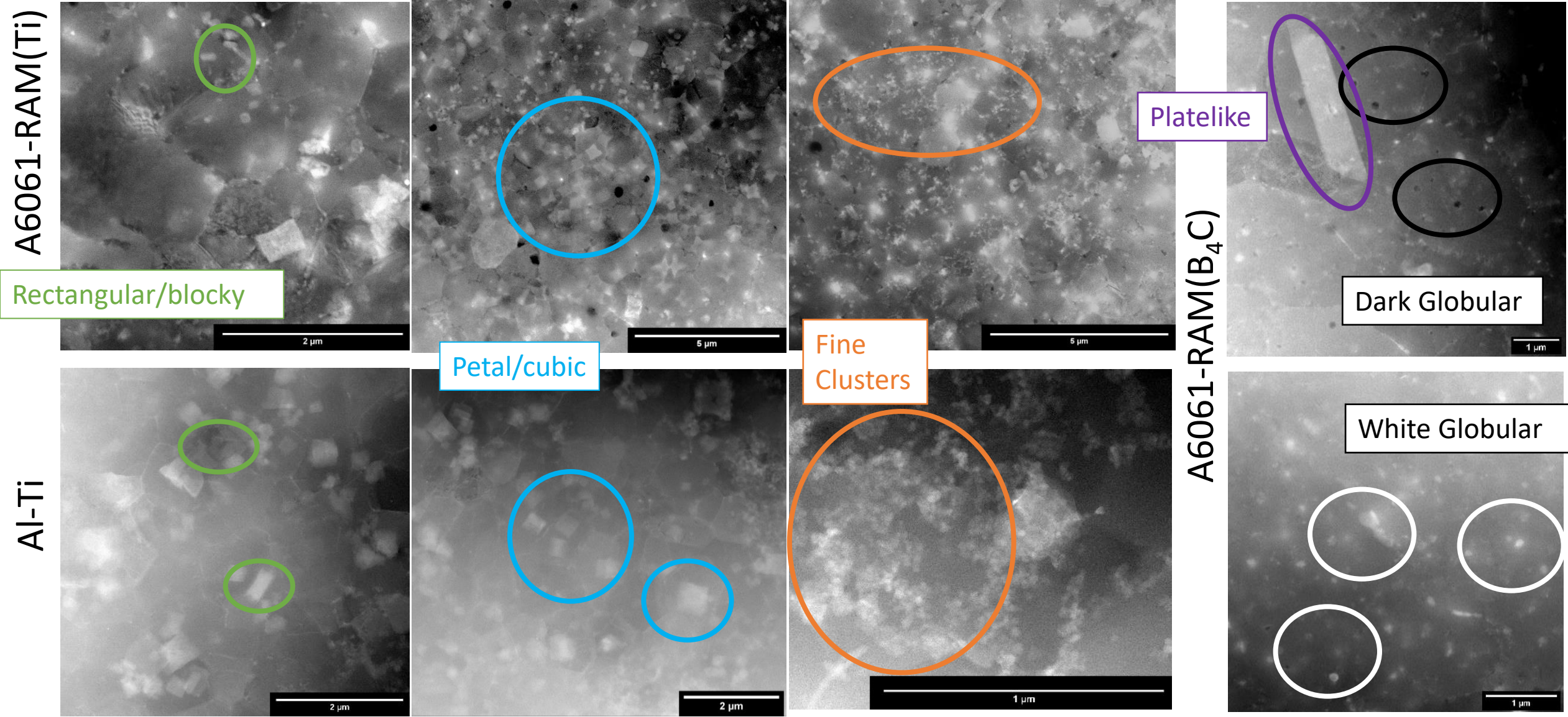
# Particle Types (XRD) For Dissolved Matrix Samples



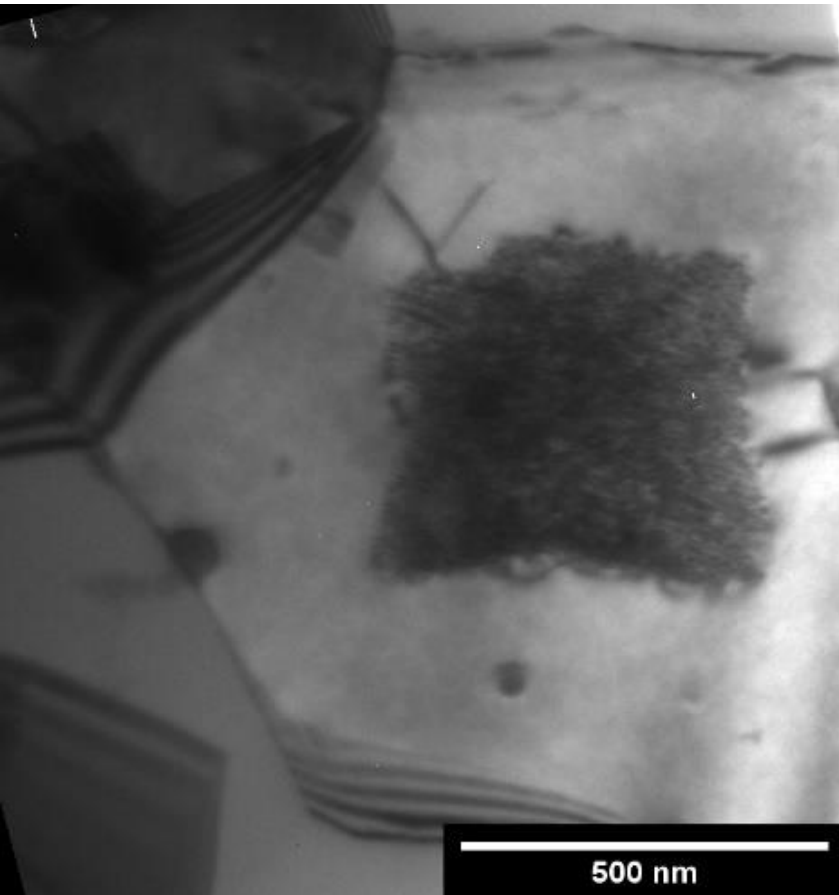
# Particle Types (XRD) For Dissolved Matrix Samples



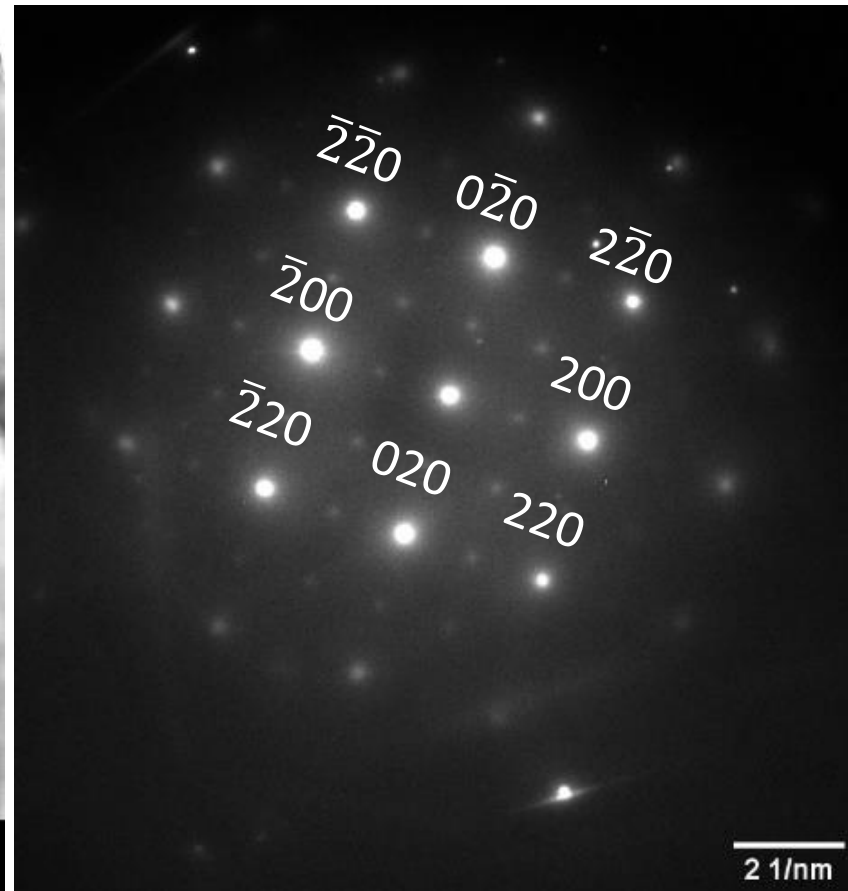
# Observed Particle Morphologies A6061-RAM(Ti), Al-Ti, & A6061-RAM(B<sub>4</sub>C) (HAADF STEM)



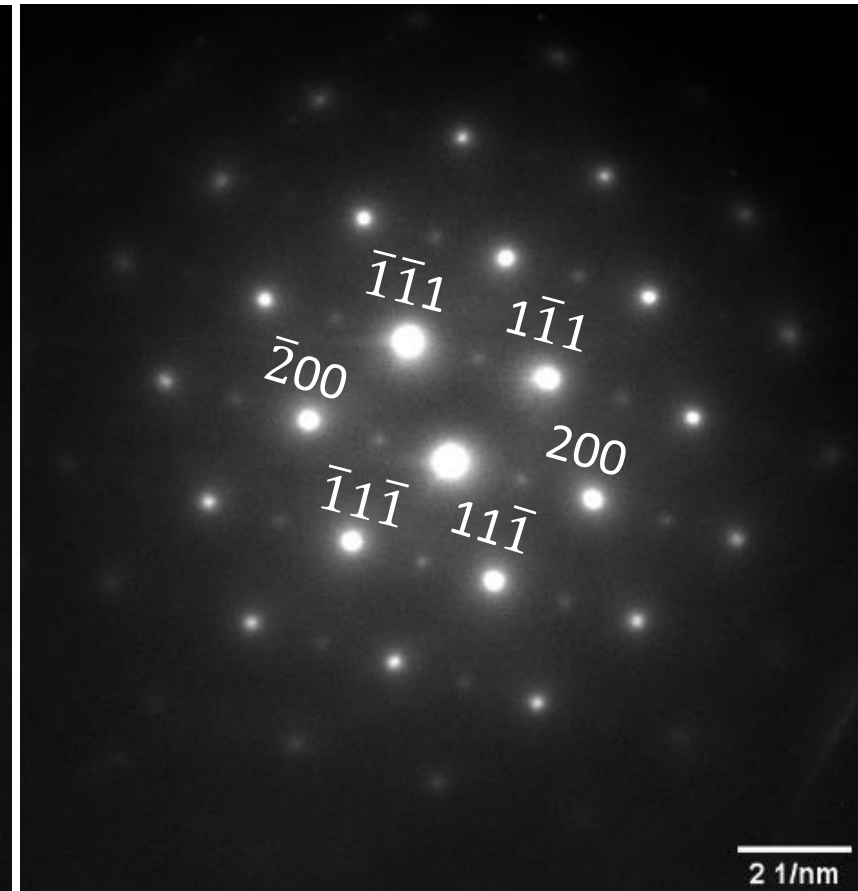
# Phase ID of Cubic/Petal Particle: Al-Ti



DF TEM image taken down center reflection of SADP

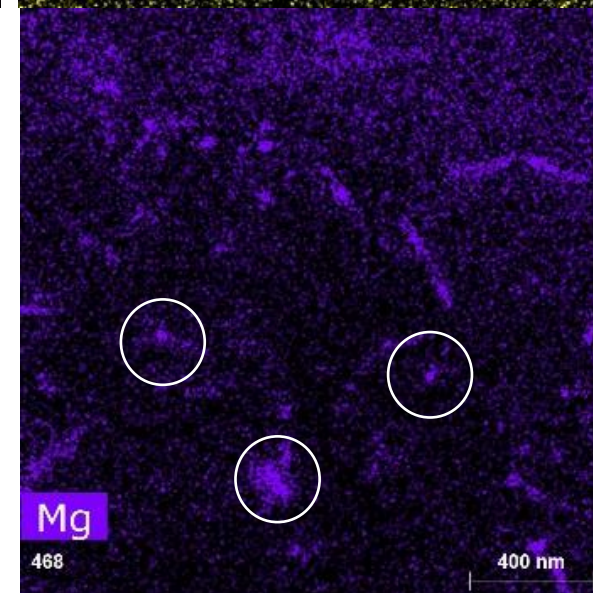
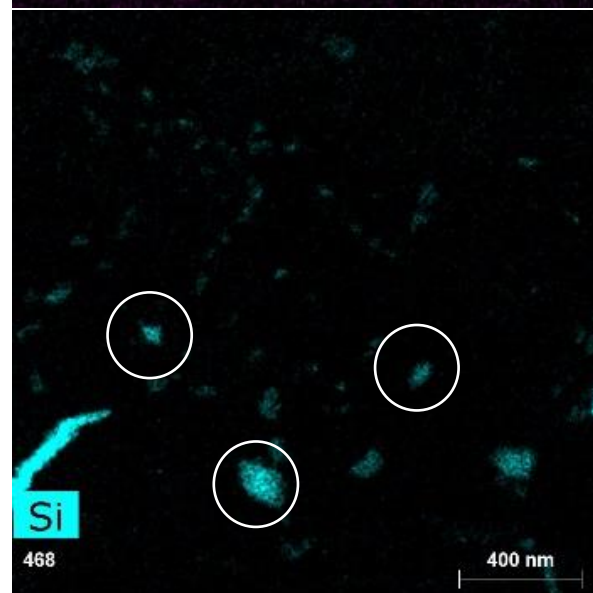
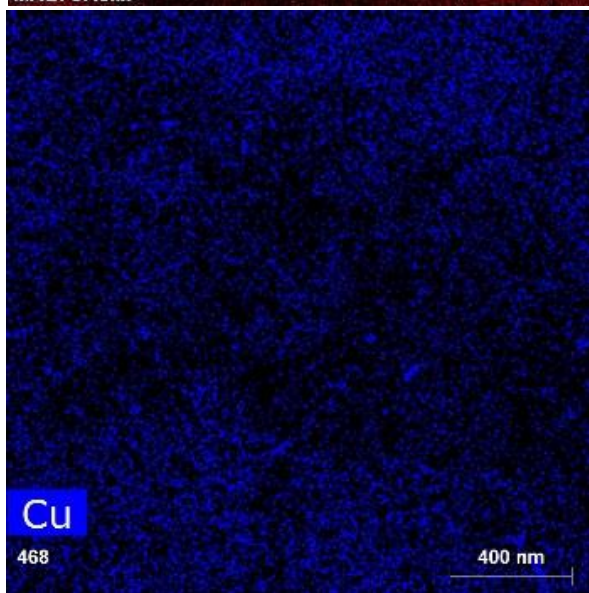
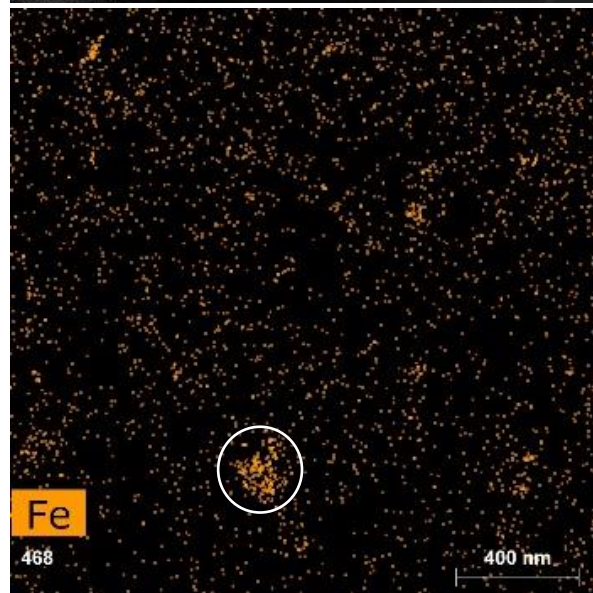
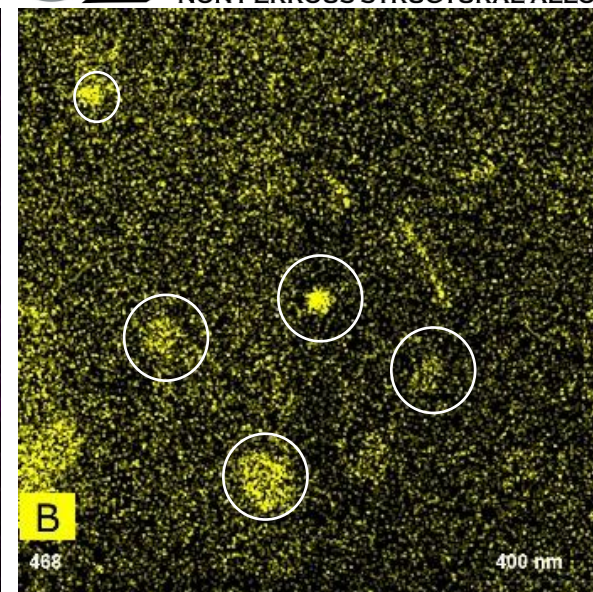
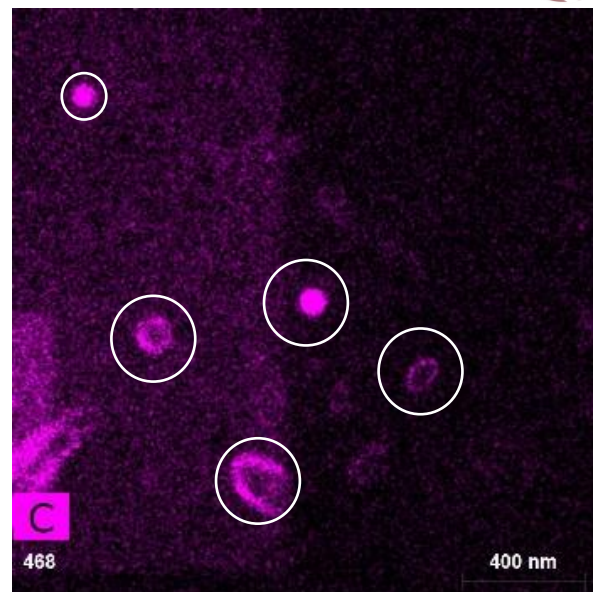
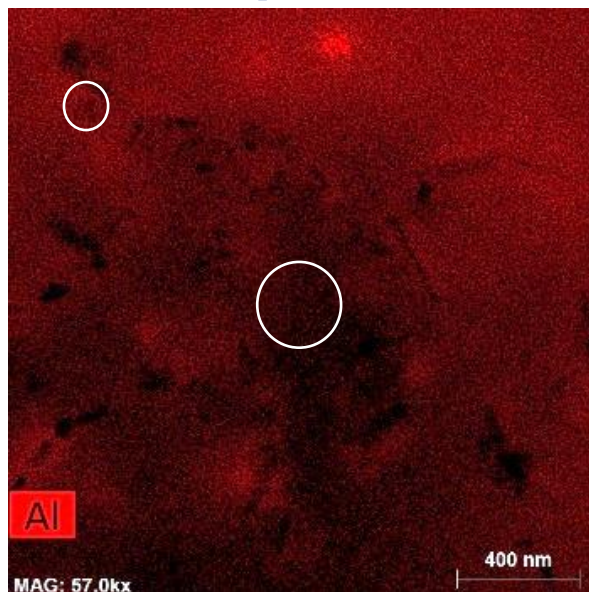
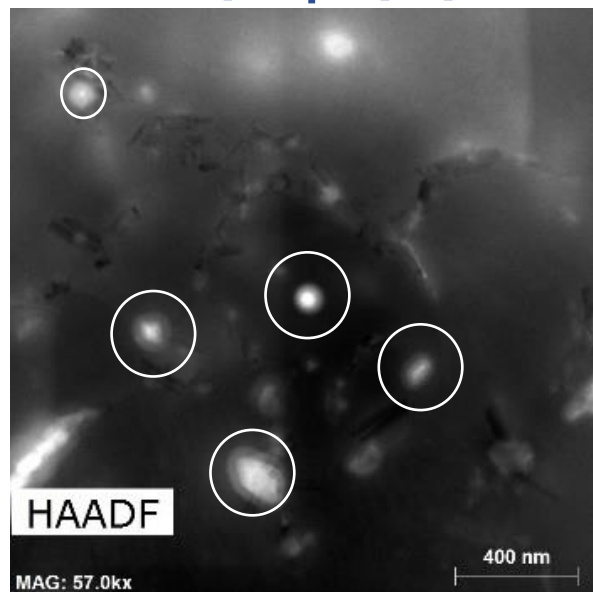


SADP from [001] zone axis



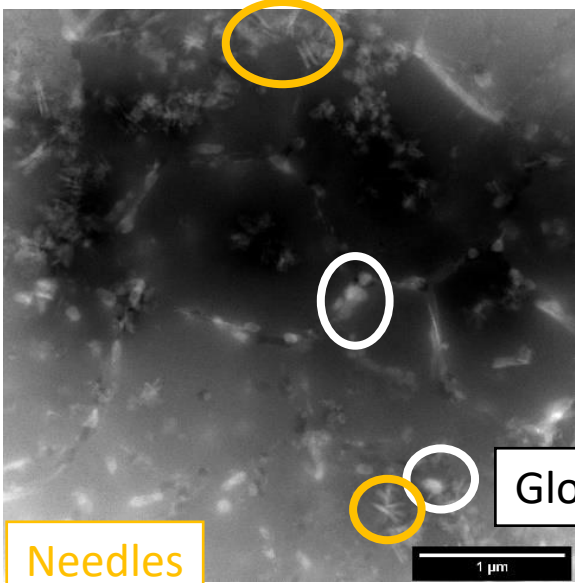
SADP from [011] zone axis

# Chemical Analysis of Particles: A6061- RAM(B<sub>4</sub>C) (STEM EDS)



# Observed Particle Morphologies A6061-RAM2 & A6061-RAM10 (HAADF STEM)

A6061-RAM2

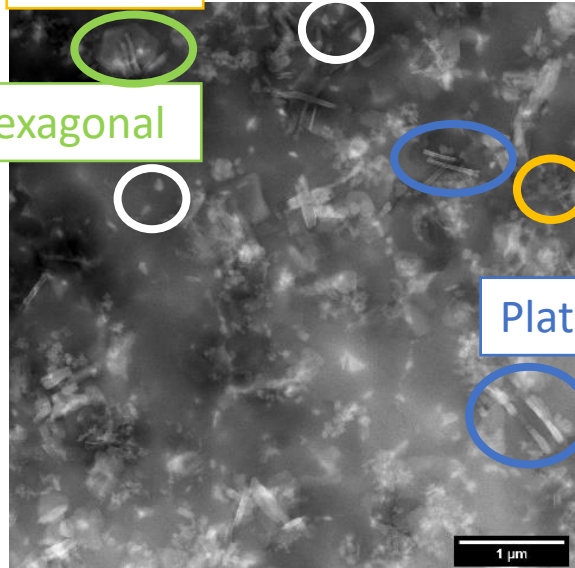


Needles

Globular

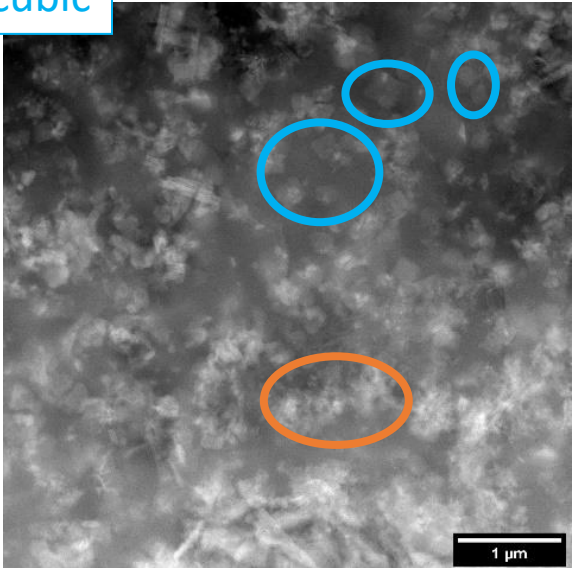
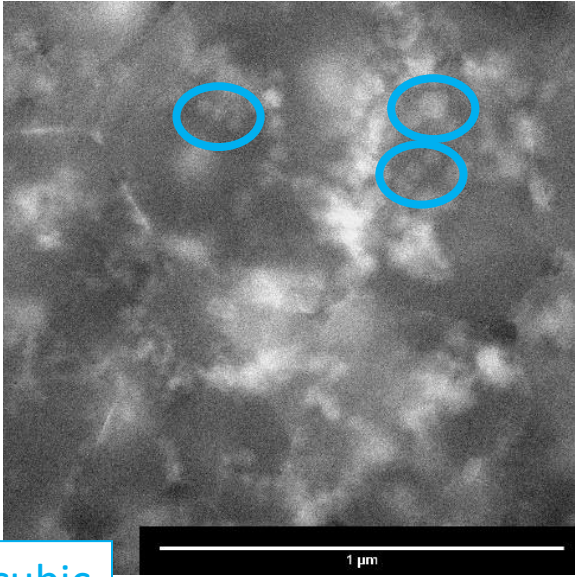
Petal/cubic

A6061-RAM10

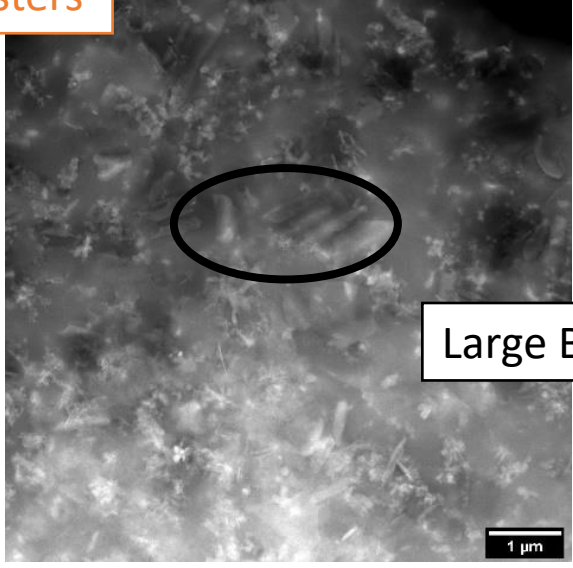
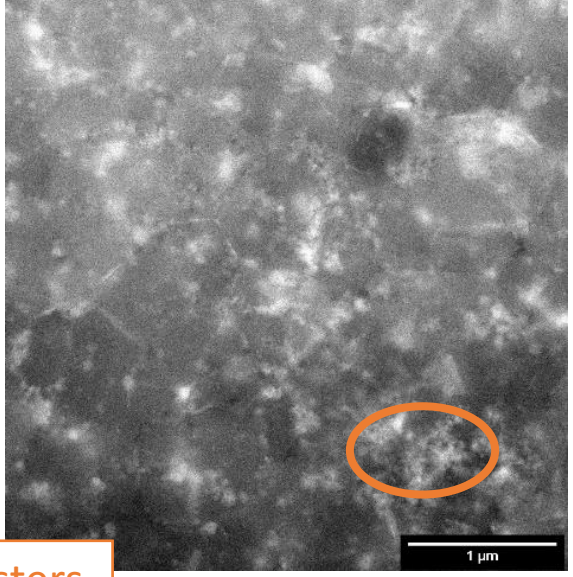


Hexagonal

Plates

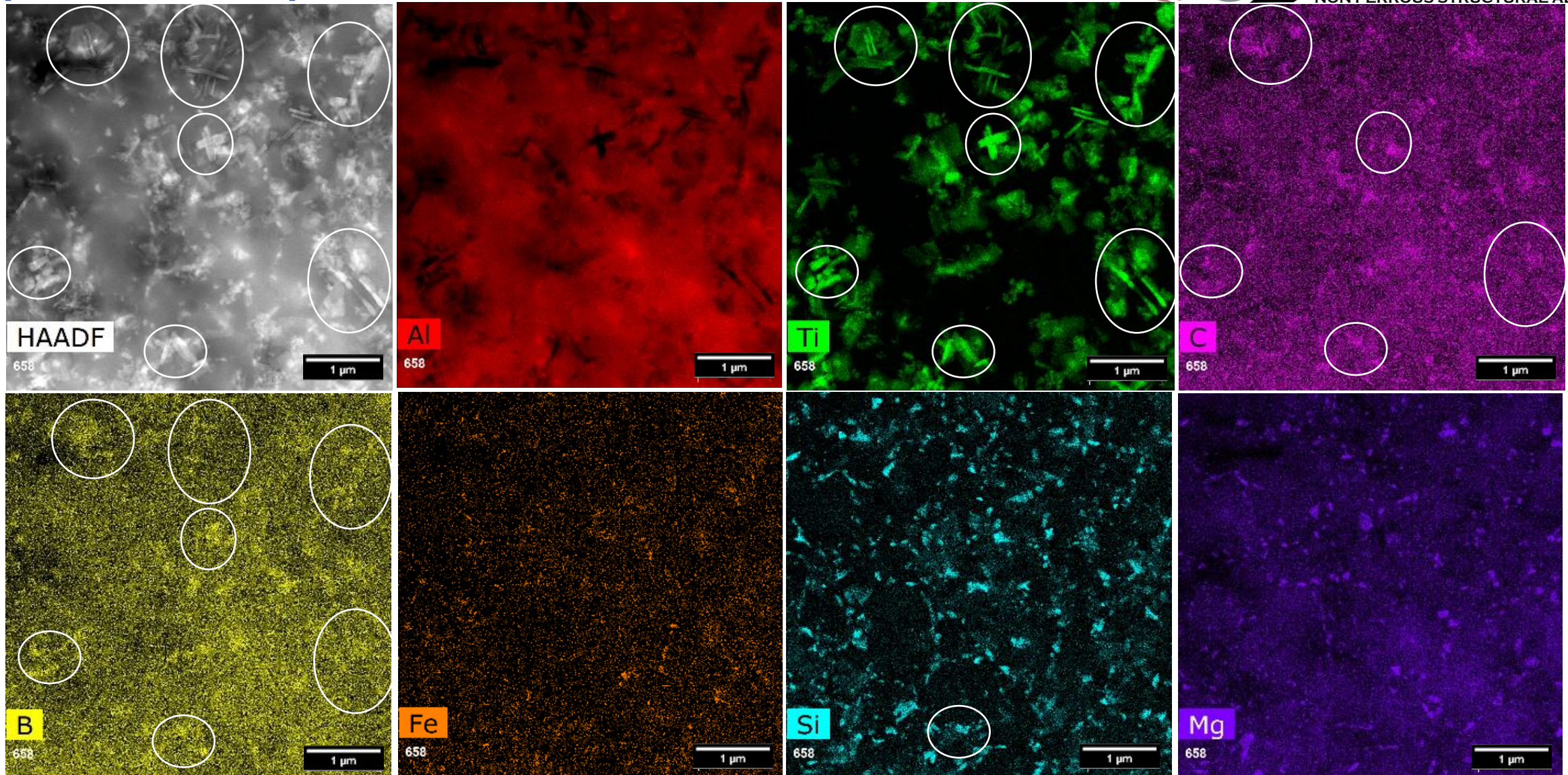


Fine Clusters



Large Blocks

# Chemical Analysis of Particles: A6061-RAM10 (STEM EDS)



## Research Question 3

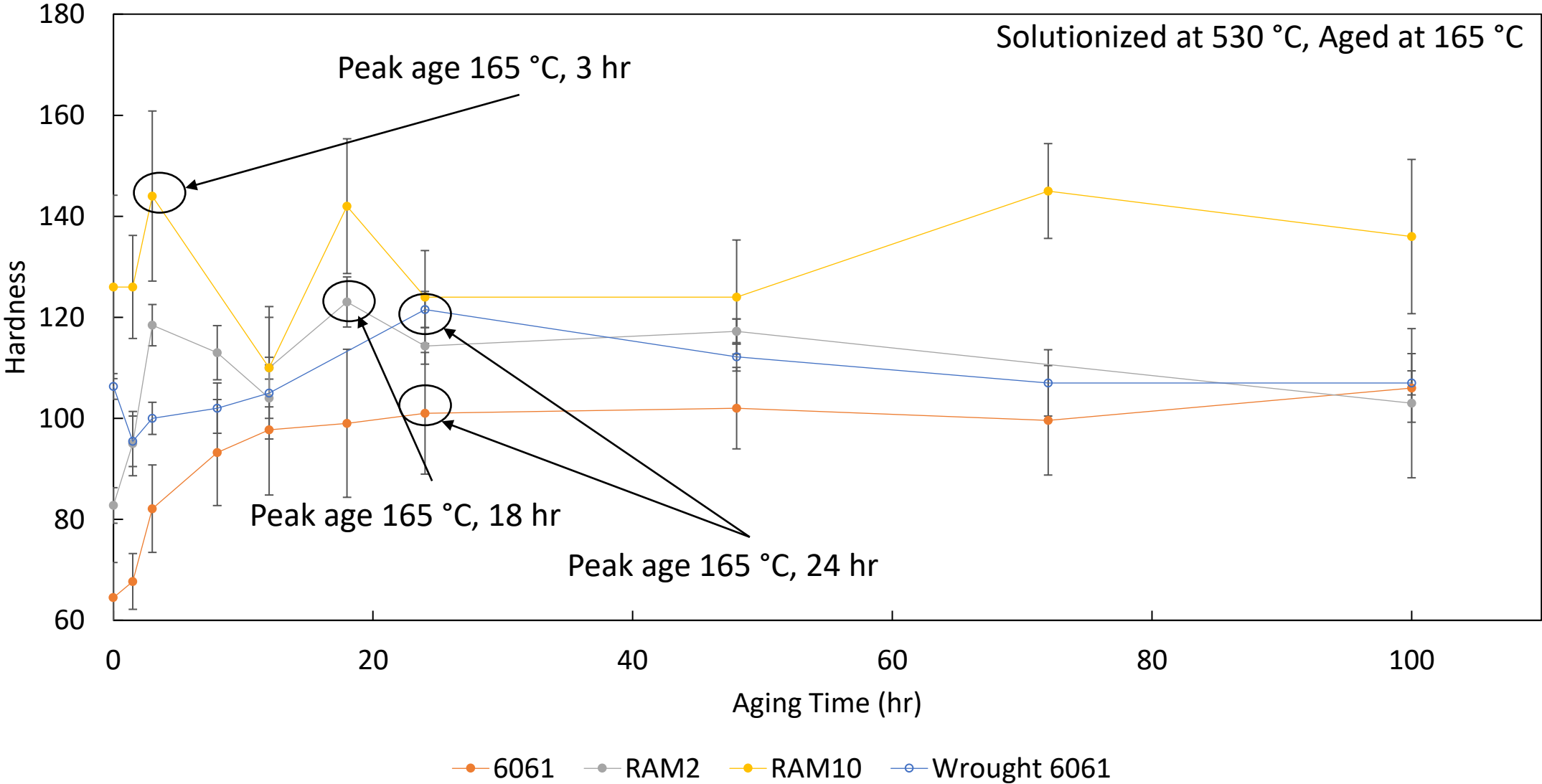
What is the impact of particle content in as-built A6061-RAM alloys, built using laser powder bed fusion, on aging and precipitation strengthening in these alloys?

Mg & Si Clusters →  $\beta''$  (nm, needle) →  $\beta'$  (rod) →  $\beta$

Solutionizing Temperature (°C)	Aging Temperature (°C)	Samples Aged in this Condition
530	150	A6061-RAM2, Wrought 6061
530	165	A6061-RAM2 & 10, Wrought 6061, AM 6061
530	175	A6061-RAM2, Wrought 6061
530	190	A6061-RAM2, Wrought 6061
500	165	A6061-RAM2, Wrought 6061



# Microhardness for All Alloys Aged at 165°C



# Microstructure of Solutionized Samples



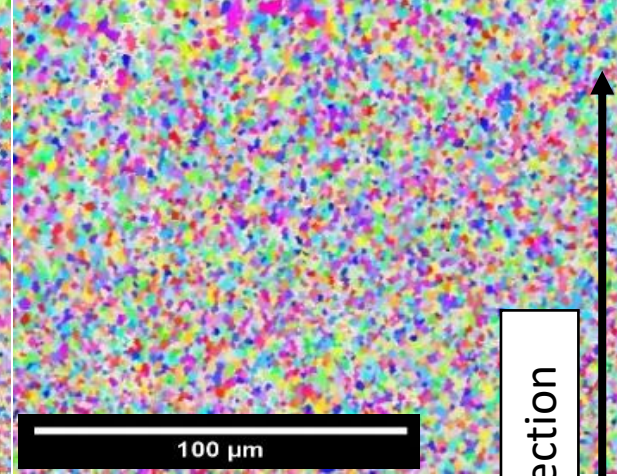
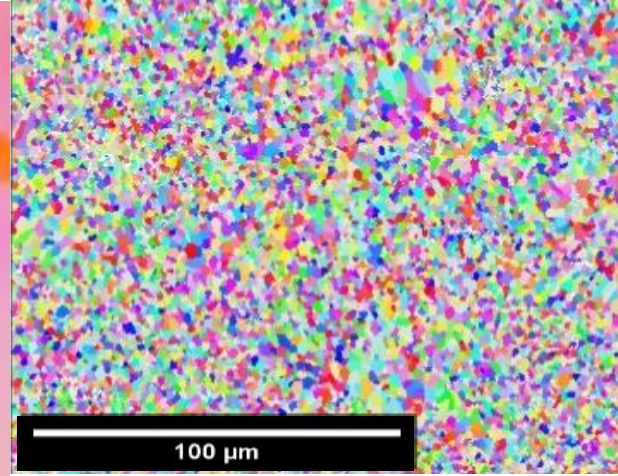
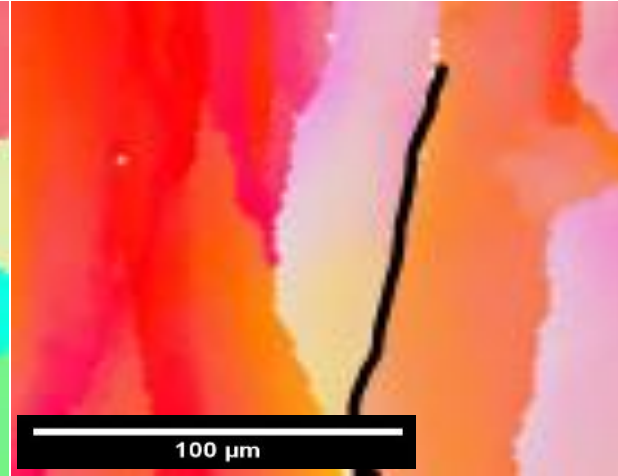
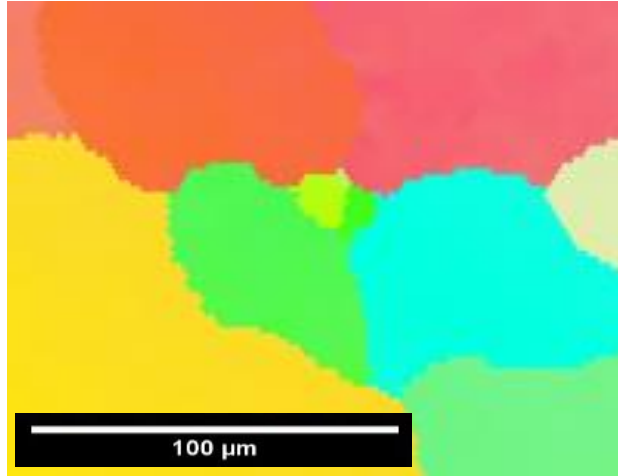
6061 Wrought

AM 6061

A6061-RAM2

A6061-RAM10

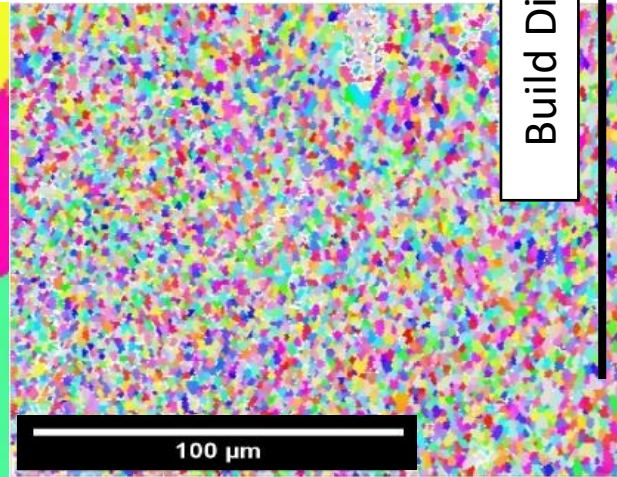
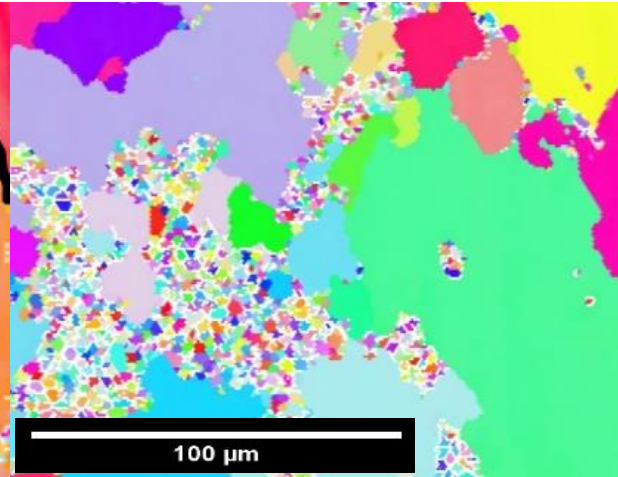
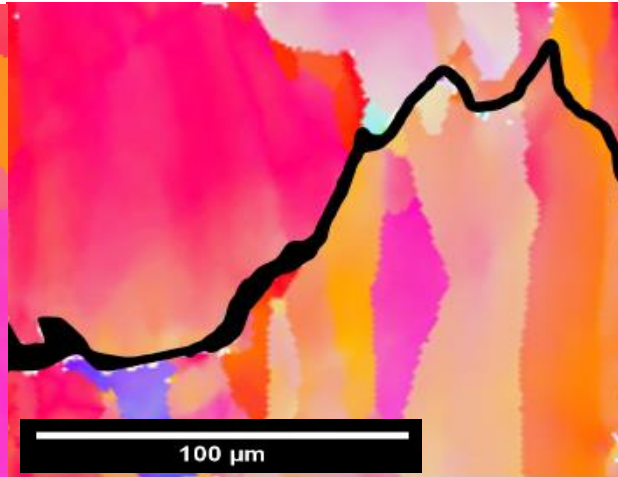
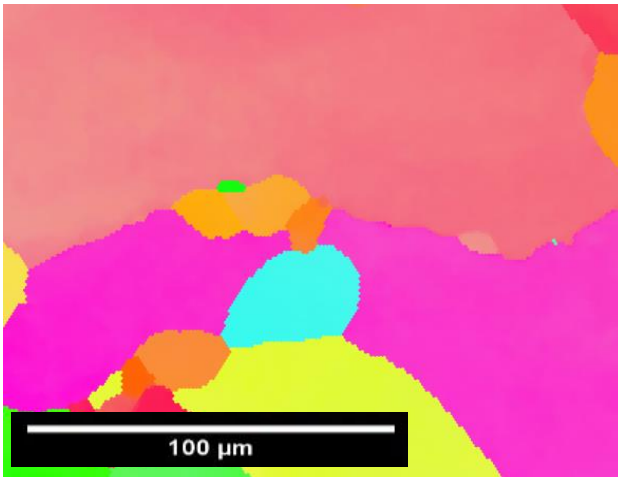
As Received/As Built



Build Direction



Solutionized at 530°C



# Microstructural Development of Aged 6061/Wrought 6061 Samples

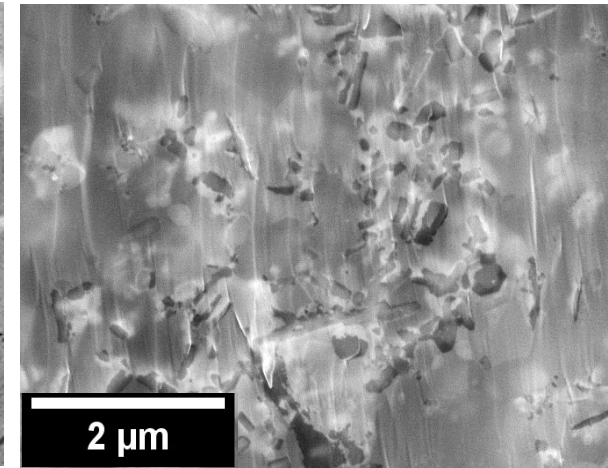
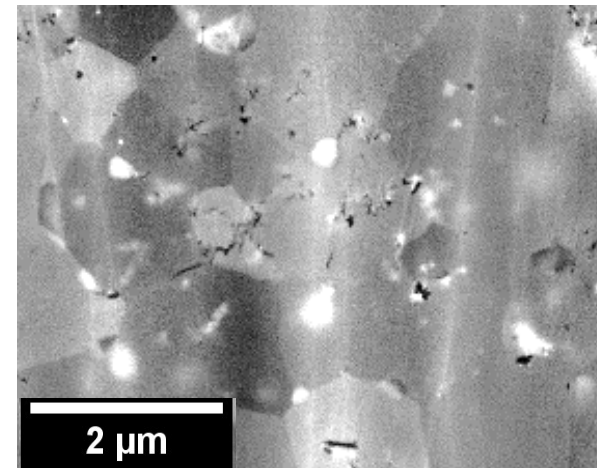
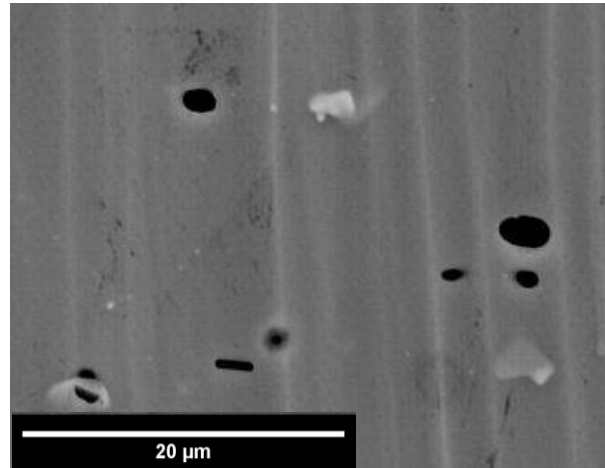
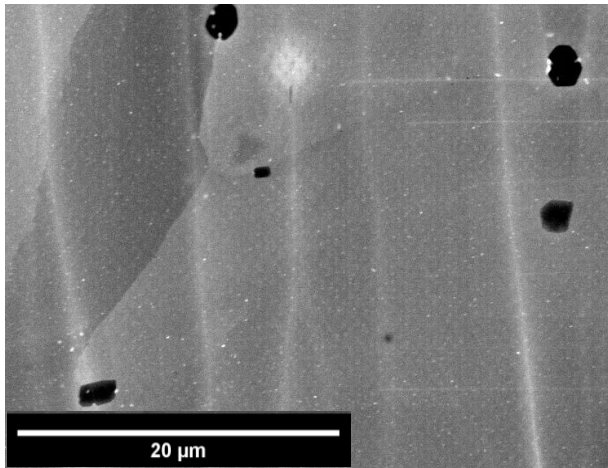
6061 AM Build

6061 Wrought

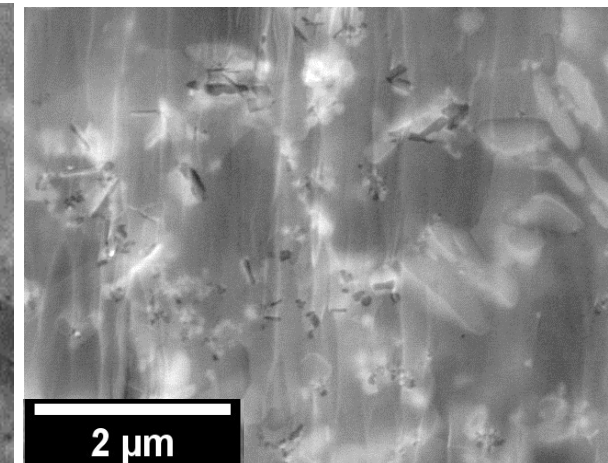
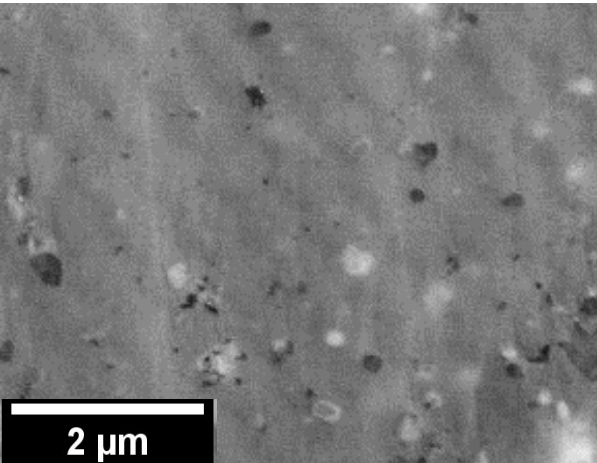
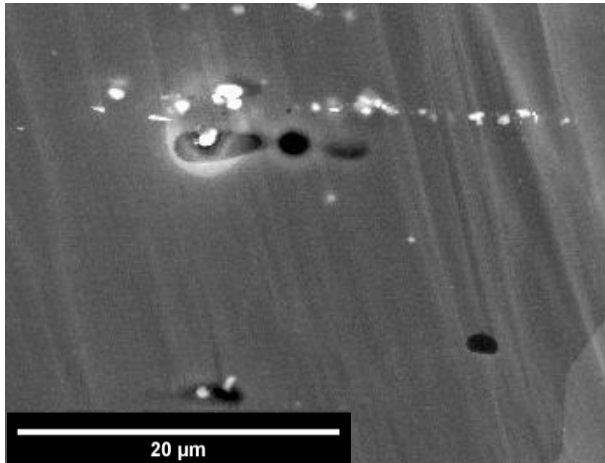
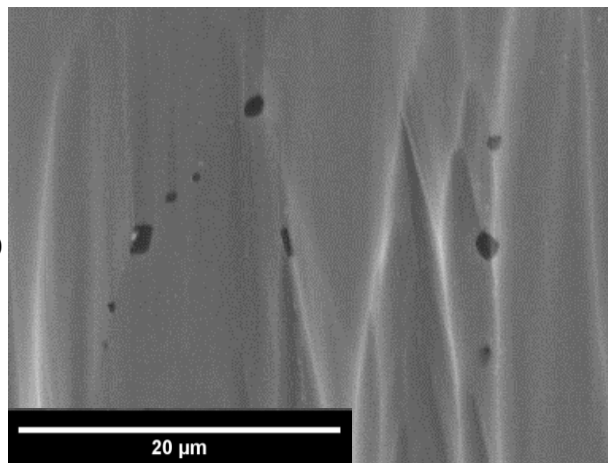
A6061-RAM2

A6061-RAM10

Peak Aged 165°C



Overaged 165°C



SEM BSE Images

# Contributions to Strengthening

- Orowan Strengthening

$$\Delta\sigma_{Orowan} = \frac{\phi G_m b}{d_p} \left( \frac{6V_p}{\pi} \right)^{\frac{1}{3}}$$

---

Contribution	Wrought 6061	AM 6061	A6061-RAM2	A6061-RAM10
Orowan (MPa)	-	-	20.9	31.0

---

# Contributions to Strengthening

- Orowan Strengthening

$$\Delta\sigma_{Orowan} = \frac{\phi G_m b}{d_p} \left( \frac{6V_p}{\pi} \right)^{\frac{1}{3}}$$

- Hall-Petch (Grain size) Strengthening

$$\Delta\sigma_y = kd^{-1/2}$$

Contribution	Wrought 6061	AM 6061	A6061-RAM2	A6061-RAM10
Orowan (MPa)	-	-	20.9	31.0
Hall-Petch, average grain size (MPa)	20.3	26.1	44.1	55.5

# Contributions to Strengthening

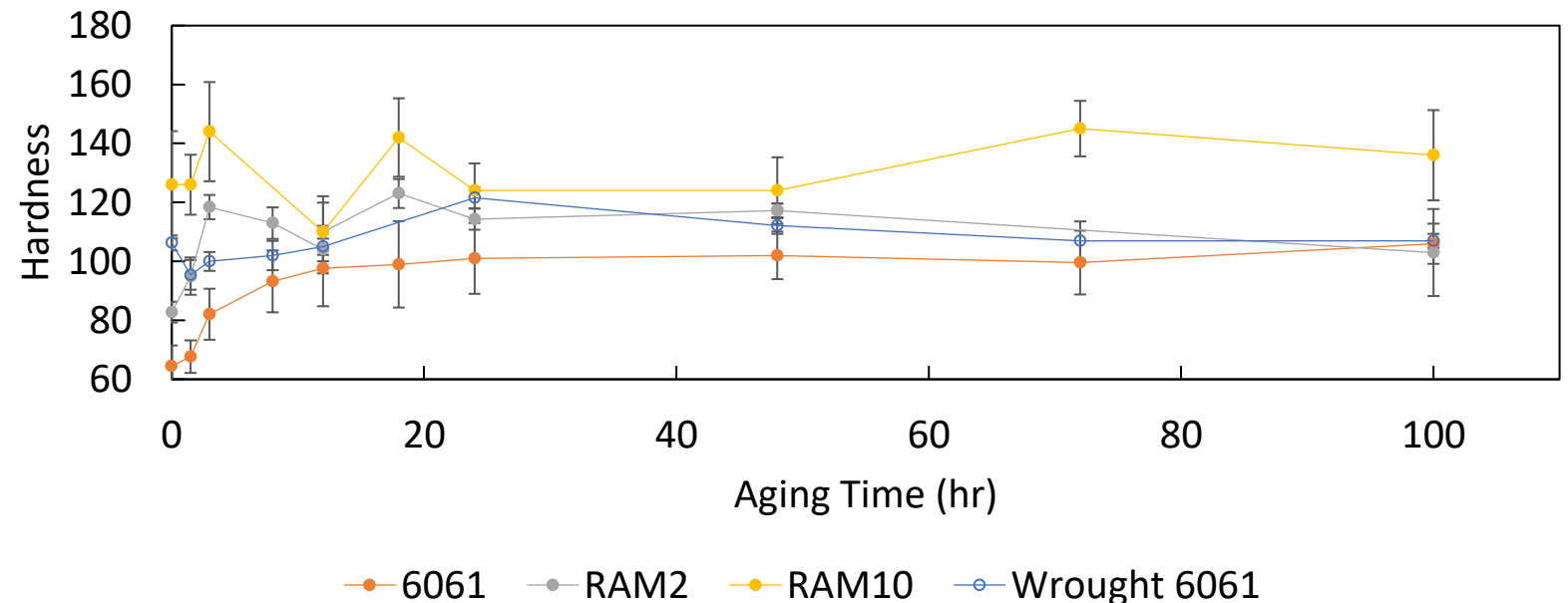
- Orowan Strengthening

$$\Delta\sigma_{Orowan} = \frac{\phi G_m b}{d_p} \left( \frac{6V_p}{\pi} \right)^{\frac{1}{3}}$$

- Hall-Petch (Grain size) Strengthening

$$\Delta\sigma_y = kd^{-1/2}$$

Contribution	Wrought 6061	AM 6061	A6061-RAM2	A6061-RAM10
Orowan (MPa)	-	-	20.9	31.0
Hall-Petch, average grain size (MPa)	20.3	26.1	44.1	55.5
Hall-Petch max grain size (MPa)	5.1	3.0	6.6	27.3



# Contributions to Strengthening

- Orowan Strengthening

$$\Delta\sigma_{Orowan} = \frac{\phi G_m b}{d_p} \left( \frac{6V_p}{\pi} \right)^{\frac{1}{3}}$$

- Hall-Petch (Grain size) Strengthening

$$\Delta\sigma_y = kd^{-1/2}$$

- Load Bearing of Reinforcing Phase

$$\Delta\sigma_{load} = 1.5V_p\sigma_i$$

Contribution	Wrought 6061	AM 6061	A6061-RAM2	A6061-RAM10
Orowan (MPa)	-	-	20.9	31.0
Hall-Petch, average grain size (MPa)	20.3	26.1	44.1	55.5
Hall-Petch max grain size (MPa)	5.1	3.0	6.6	27.3

# Summary & Conclusions

- For the laser parameters studied in in-situ imaging, all A6061-RAM2 melts achieved same level of refinement (avg. grain size  $\sim 2\text{-}3\ \mu\text{m}$ ) and show no signs of hot tearing
- Addition of Ti and/or  $\text{B}_4\text{C}$  refines microstructure compared to 6061, full refinement achieved in A6061-RAM2, A6061-RAM10, and A6061-RAM(Ti) and smallest grain size in A6061-RAM(Ti)
  - SiC, Ti borides and carbides, and  $\text{Al}_3\text{Ti}$  down to  $\sim 100\ \text{nm}$  all served as inoculants,  $\text{Al}_3\text{Ti}$  refining most effectively for amount of initial reactive particles
  - Imply wider range of inoculant types and sizes can be used in AM vs. casting, and wider design space for consideration of which particle content and type could be used to achieve certain mechanical properties
  - Shape of refined regions in samples with CET suggest refinement is less dependent on solidification conditions and more dependent on where reactant particles, and thus solute, is distributed in the melt
- Formation of  $\text{Mg}_2\text{Si}$  precipitates during aging increases hardness of all alloys, however nucleation sites in all alloys studied (with a higher amount observed in RAM alloys) leads to coarser particles than expected  $\beta''$  strengthening precipitate
- Orowan and Hall-Petch strengthening were estimated to have a large contribution towards strength in the A6061-RAM alloys and most likely account for the higher hardness values, with Hall-Petch providing more significant contribution



## Questions?

Thank you for listening!  
[chloe@elementum3d.com](mailto:chloe@elementum3d.com)